

ZhongPing Lee
Xiamen University

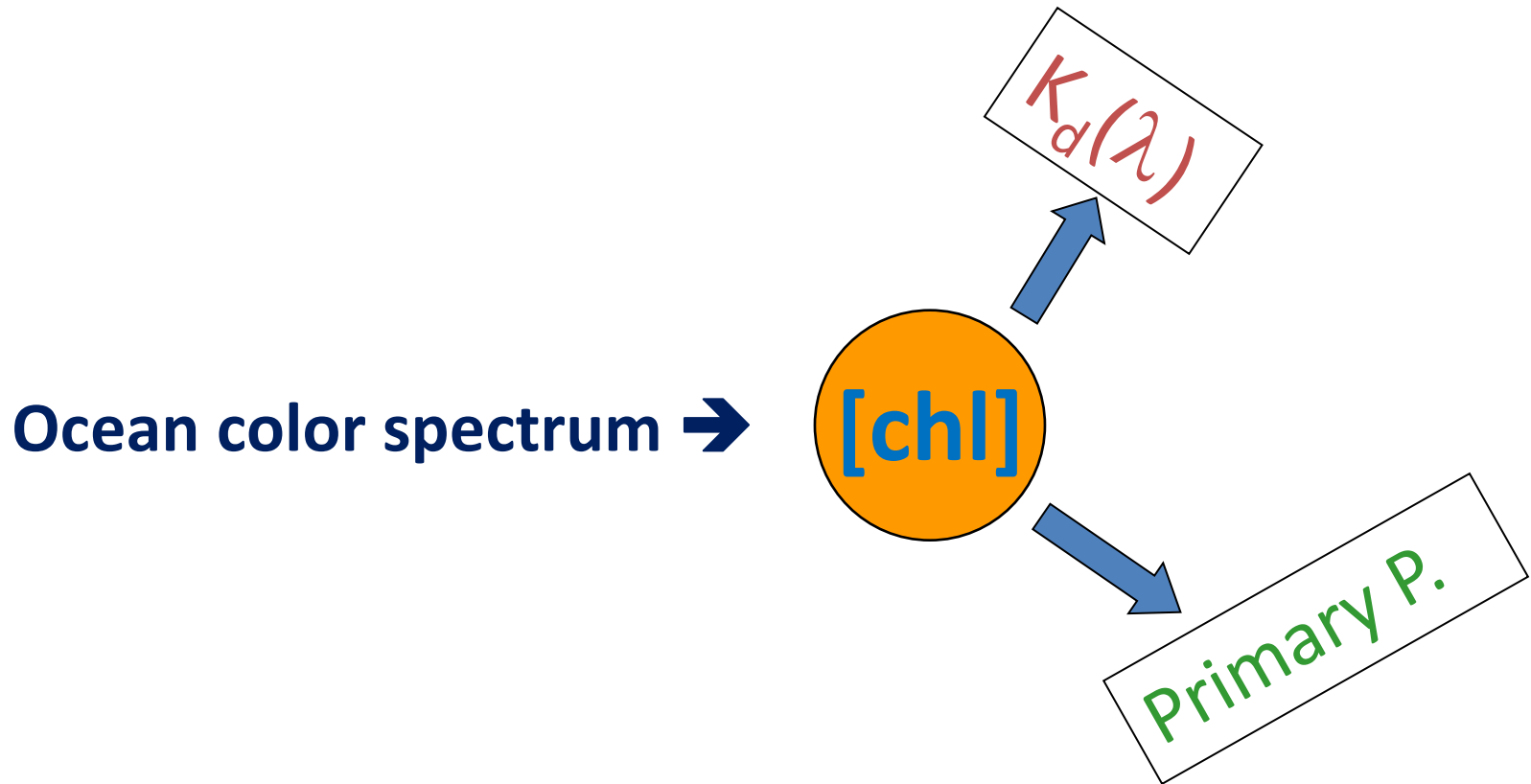
Inherent Optical Properties (IOPs)

Lecture 3: Applications

$R_{rs}(\lambda)$  **IOPs**

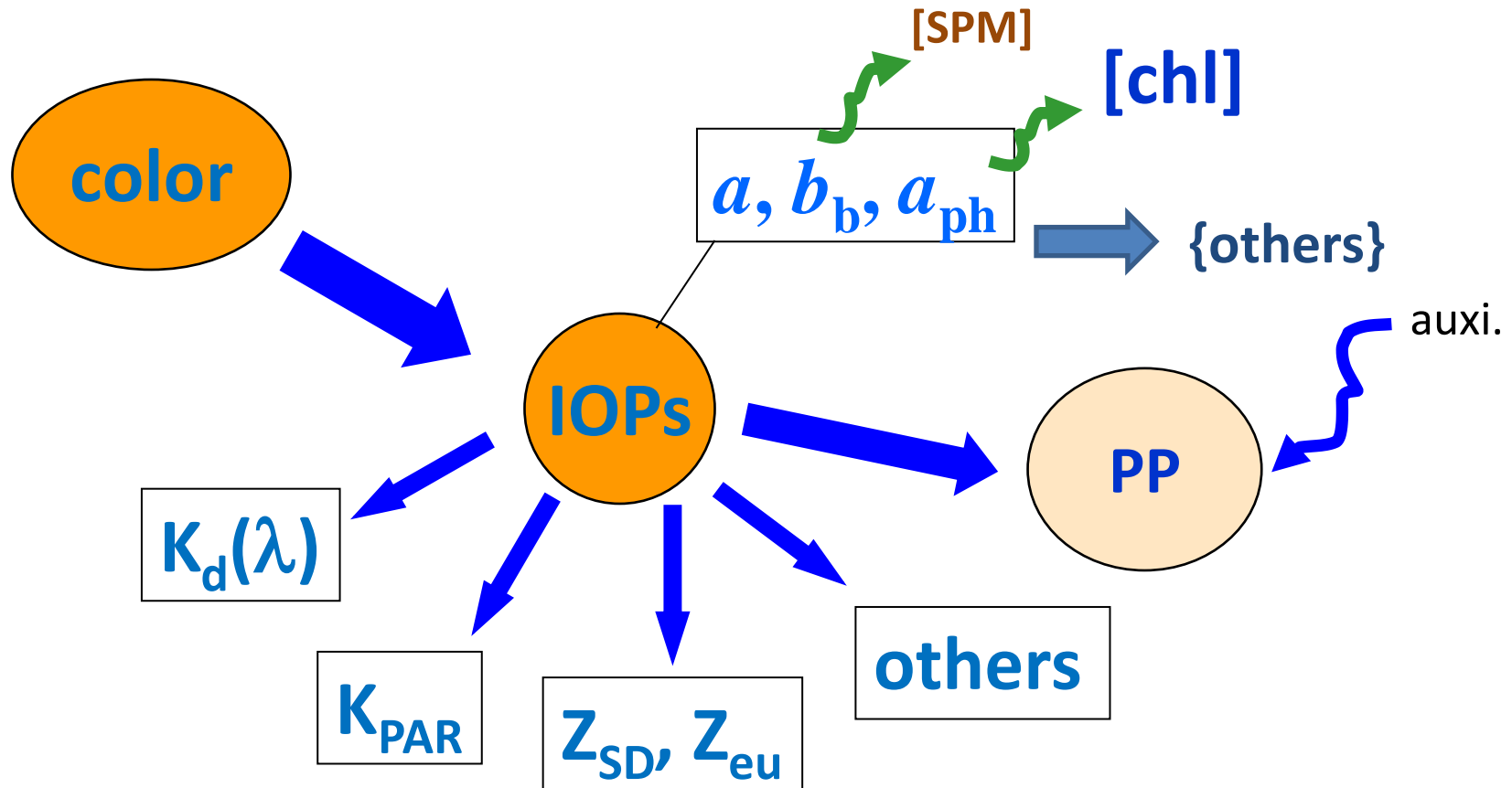
What to do with the retrieved IOPs?

Traditional strategy: [chl] centered system



Works for waters "Case-1" waters (where IOPs co-vary with [Chl]).

IOP-centered system:



No division of "Case-1" vs "Case-2" waters.

- 1. Estimation of diffuse attenuation coefficient ($K_d(\lambda)$)**
- 2. Estimation of $K_d(\text{PAR})$ and euphotic-zone depth**
- 3. Estimation of water clarity (Secchi disk depth)**
- 4. Estimation of primary production**
- 5. A few other examples**

1. Estimation of diffuse attenuation coefficient ($K_d(\lambda)$)

Traditionally,

$$K_d(490) = A \left(\frac{L_w(\lambda_{blue})}{L_w(\lambda_{green})} \right)^B$$

Austin and Petzold (1981)

Or,

$$K_d(\lambda, [Chl]) = K_w(\lambda) + \chi(\lambda)[Chl]^{e(\lambda)} \quad (2)$$

(Morel and Maritorena 2001)

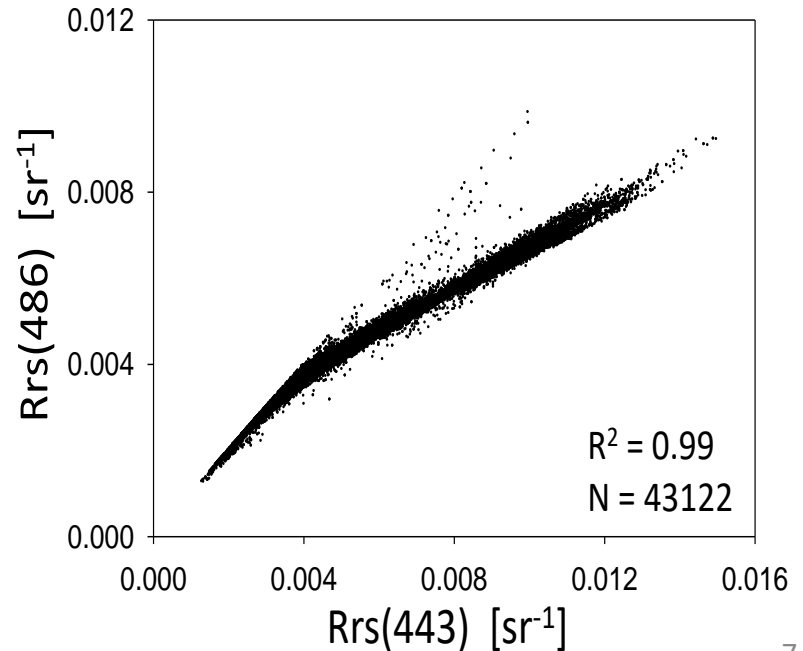
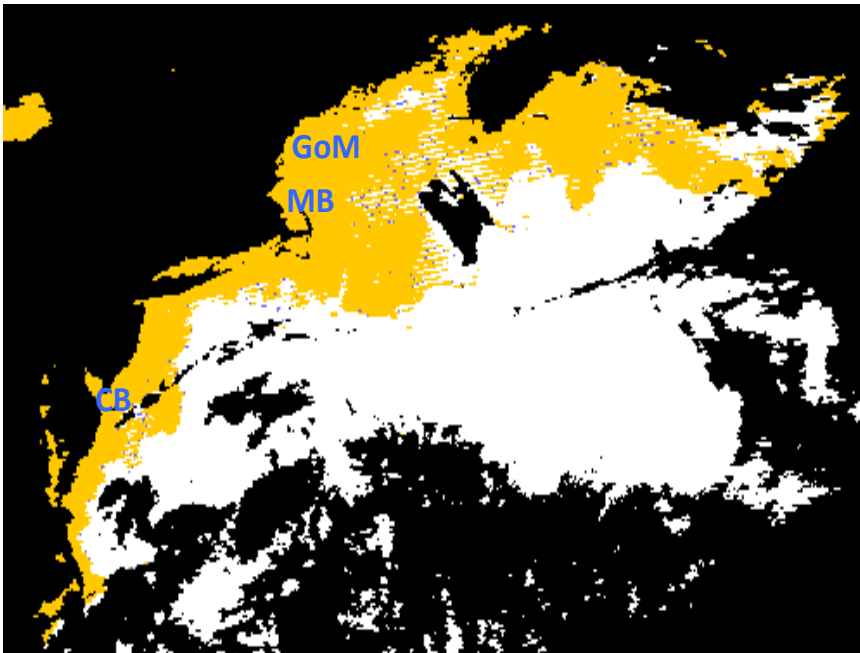
For “Case-1” waters

$$\log_{10}(K_{bio}(490)) = a_0 + \sum_{i=1}^4 a_i \log_{10} \left(\frac{R_{rs}(\lambda_{blue})}{R_{rs}(\lambda_{green})} \right)$$

$$Kd_{490} = K_{bio}(490) + 0.0166$$

$$\log_{10}(chlor_a) = a_0 + \sum_{i=1}^4 a_i \log_{10} \left(\frac{R_{rs}(\lambda_{blue})}{R_{rs}(\lambda_{green})} \right)^i$$

$$Rrs(\lambda_{blue}) = Rrs(443) > Rrs(486)$$





The standard $K_d(490)$ and Chl products are 100% co-vary in **coastal waters**; further...

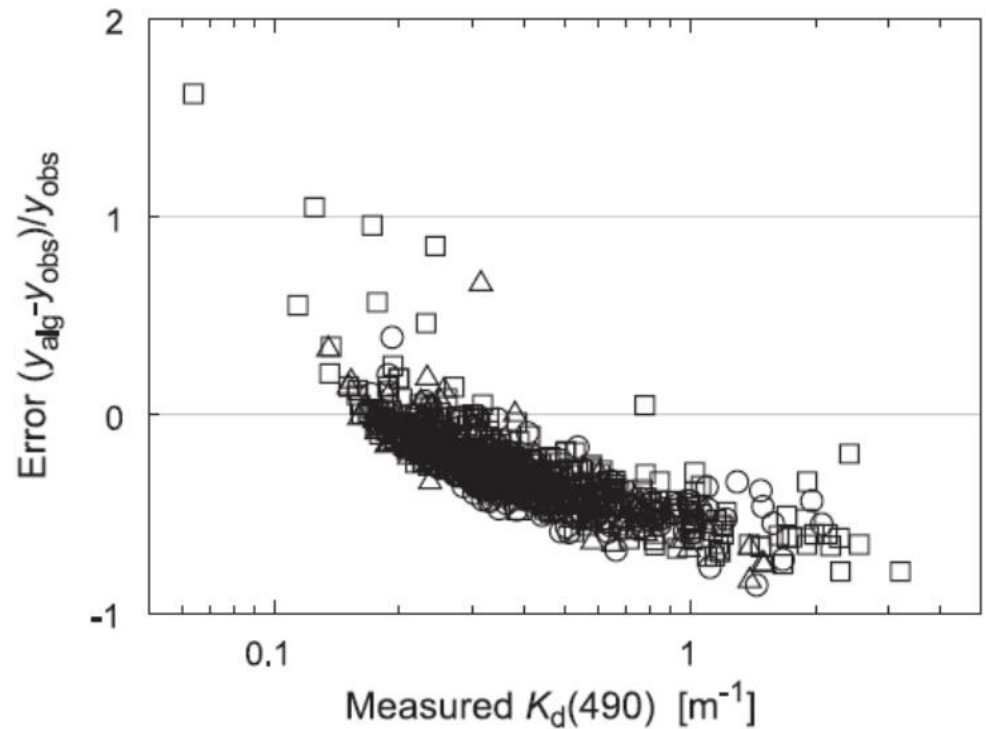
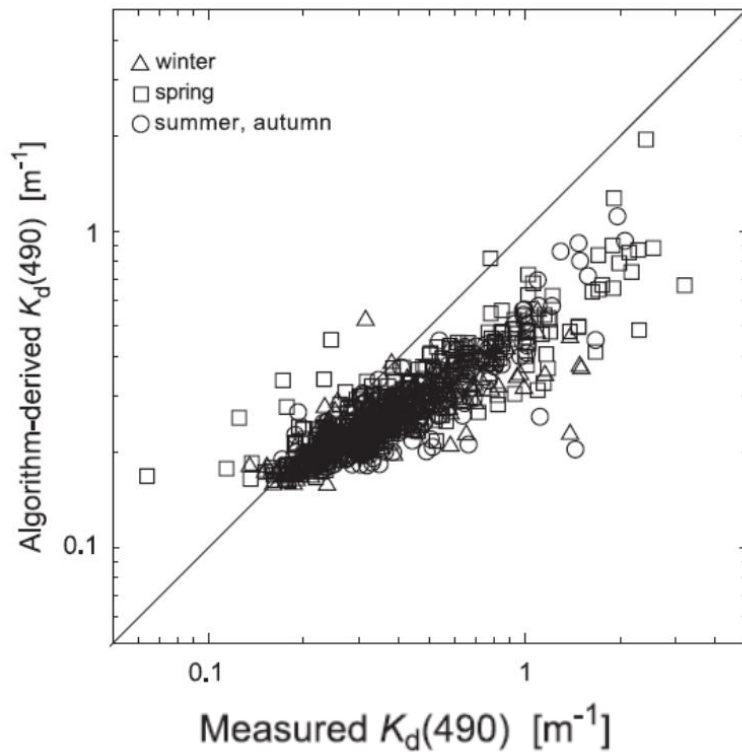
$$K_d(490) = Fun\left(\frac{R_{rs}(490)}{R_{rs}(555)}\right)$$

AOP: sun angle dependent

Nearly independent of sun angle

The two sides do **not** match in optical nature.

In addition, ratio-derived K_d has large uncertainties



(Darecki and Stramisk, 2004)

How to estimate $K_d(\lambda)$ from IOPs?

What is the analytical relationship between K_d and IOPs?

Through Monte Carlo simulations:

$$K_d = \frac{a}{\cos(\theta_0)} \sqrt{1 + (0.425 \cos(\theta_0) - 0.19) \frac{b}{a}} \quad (\text{Kirk 1984})$$

$$K_d(0) = \frac{1.04(a + b_b)}{\cos(\theta_0)} \quad (\text{Gordon 1989})$$

Relationship based on radiative transfer?

$$\cos(\theta) \frac{dL}{dz} = -cL + \int_{4\pi} L(\theta', \varphi') \beta(\theta' \rightarrow \theta, \varphi' \rightarrow \varphi) dw'$$

(inelastic scattering omitted)

Integrate over the downwelling hemisphere:

(Aas, 1987)

$$\int_{2\pi_d} \cos(\theta) \frac{dL}{dz} dw = \int_{2\pi_d} \left(-cL + \int_{4\pi} L(\theta', \varphi') \beta(\theta' \rightarrow \theta, \varphi' \rightarrow \varphi) dw' \right) dw$$

Left side:

$$\int_{2\pi_d} \cos(\theta) \frac{dL}{dz} dw = \frac{d}{dz} E_d$$

1st term on the right side:

2nd term on the right side:

$$\int_{2\pi_d} cL dw = cE_{od} \quad \int_{2\pi_d} \left(\int_{4\pi} (...) dw \right) dw' = (b - r_d b_b) E_{od} + r_u b_b E_{ou}$$

$$\frac{dE_d(z)}{dz} = -\frac{a}{\mu_d(z)} E_d(z) - \frac{r_d(z) b_b}{\mu_d(z)} E_d(z) + \frac{r_u(z) b_b}{\mu_u(z)} E_u(z)$$

$$-\frac{dE_d(z)}{E_d(z) dz} = \frac{a}{\mu_d(z)} + \frac{r_d(z) b_b}{\mu_d(z)} - \frac{r_u(z) b_b}{\mu_u(z)} R \quad R = \frac{E_u}{E_d}$$

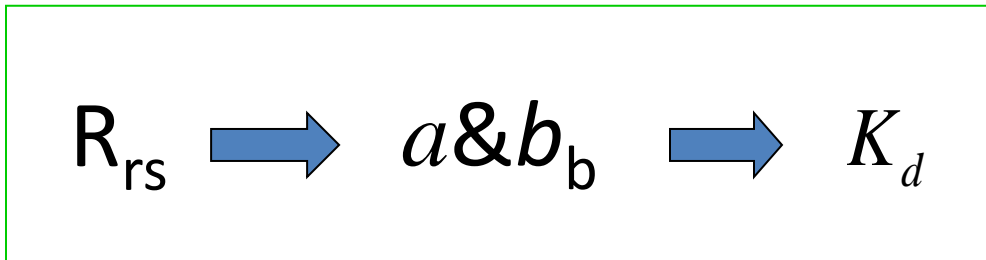
$$K_d(\lambda, z) = -\frac{d E_d(\lambda, z)}{E_d(\lambda, z) dz}$$

$$K_d = \frac{a}{\mu_d} + \left(\frac{r_d}{\mu_d} - \frac{r_u R}{\mu_u} \right) b_b$$

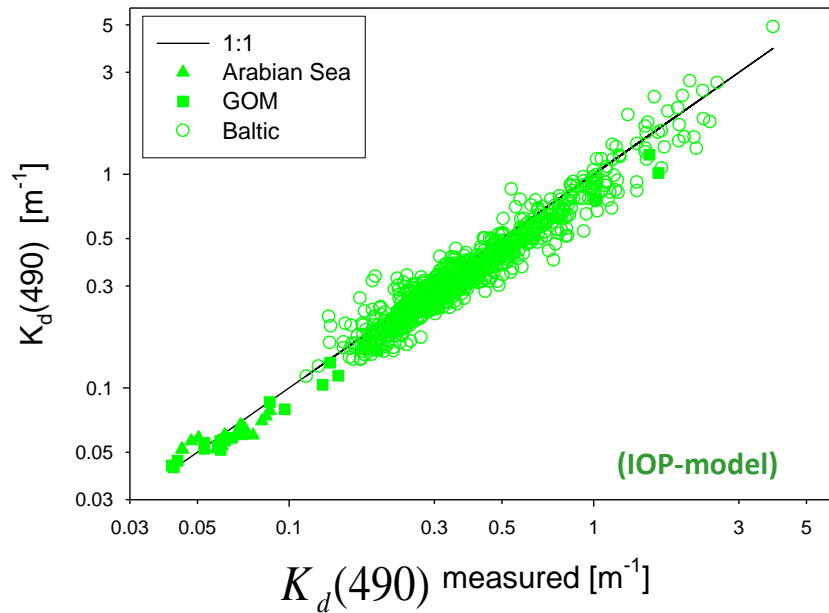
$$K_d = m_0 a + v b_b \quad v \neq m_0$$

$$v = m_1 (1 - m_2 e^{-m_3 a}) \quad (\text{Lee et al. 2005, 2013})$$

($m_{0,1,2}$ are wavelength independent)

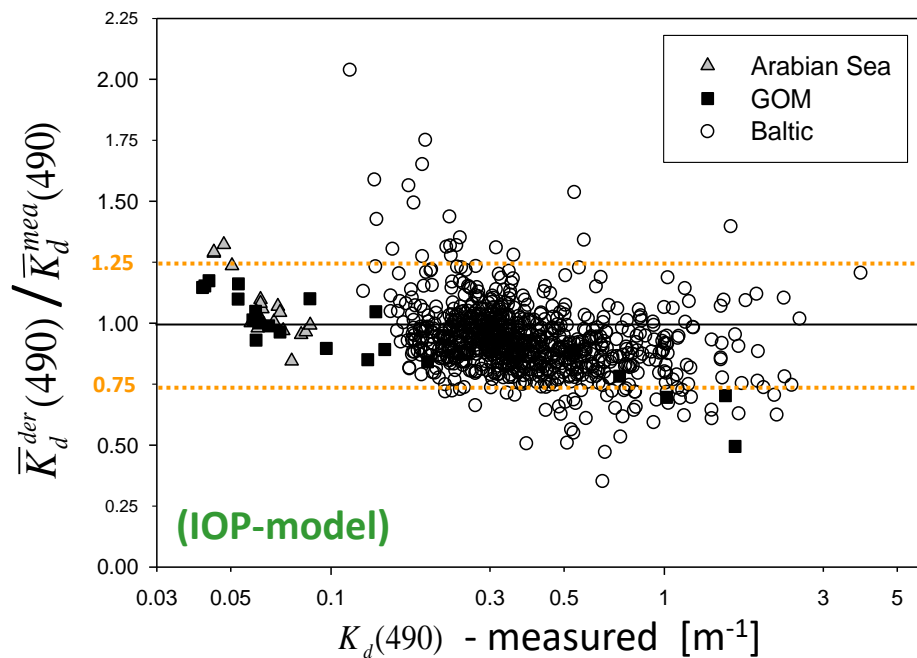


No division of “Case 1” vs “Case 2” waters.

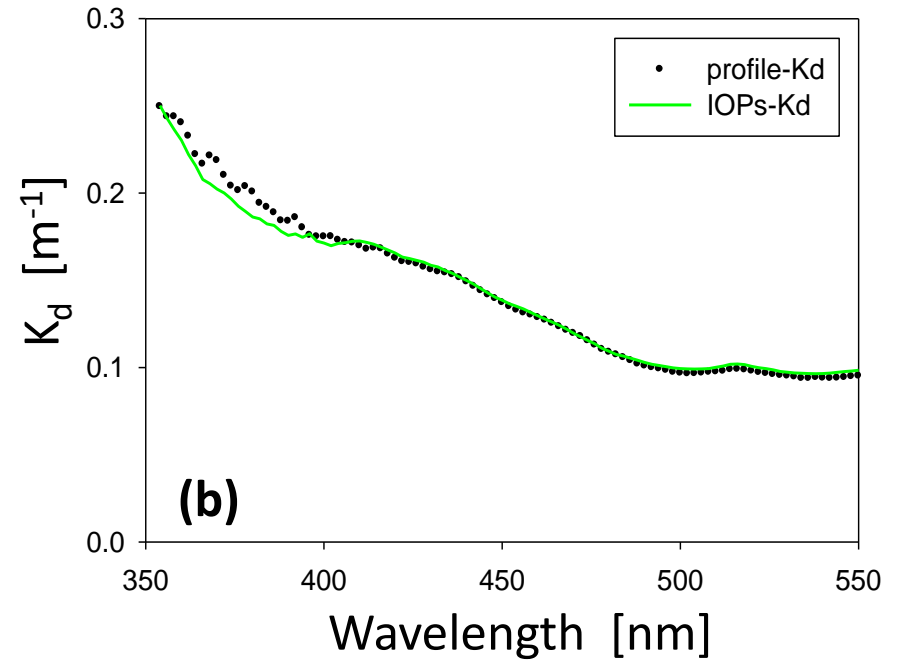
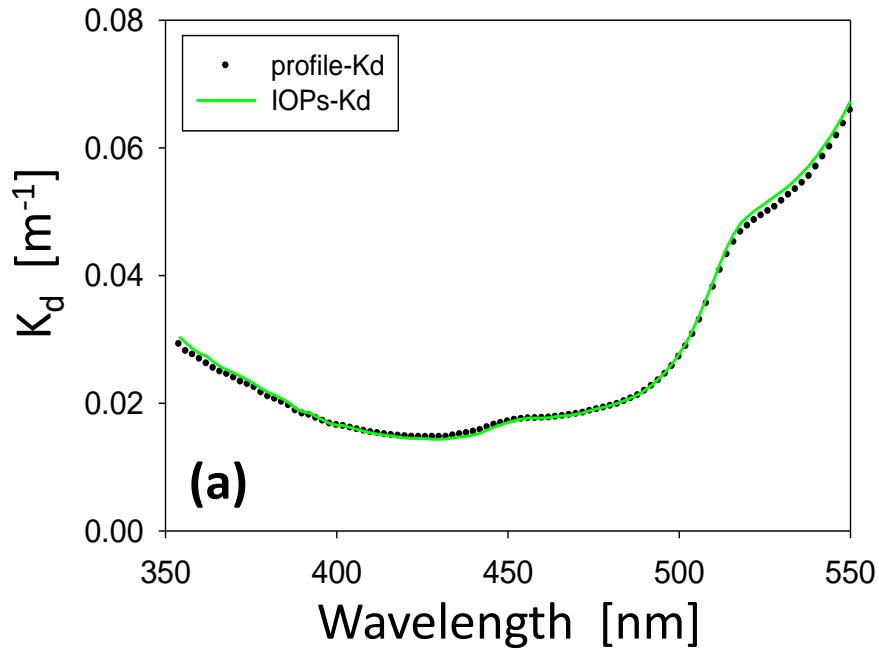


Oceanic & Coastal waters

(Lee et al. 2005)



K_d spectrum:



(Lee et al 2013)

2. Estimation of K_{PAR} and euphotic-zone depth

$$PAR(z) = PAR(0) e^{-K_{\text{PAR}} z}$$

$$K_{\text{PAR}} = K_w + k_c C + K_x$$

Good for earlier days,
Not good for the 21st century

hence of K_{PAR} .

1. K_w is a value averaged over the whole spectrum. It is computed for a layer extending from zero to a certain depth Z within an ideally optically pure ocean. When computing this depth-averaged value, denoted $\bar{K}_w(0, Z)$, the spectral distribution of the light at the surface, $E_0(\lambda)$, and at the depth Z , $E_z(\lambda)$, intervenes according to

$$\bar{K}_w(0, Z) = -Z^{-1} \log \left\{ \frac{\int_{400}^{700} E_0(\lambda) \exp[-K_w(\lambda)Z] d\lambda}{\int_{400}^{700} E_0(\lambda) d\lambda} \right\} \quad (7)$$

In other words, $\bar{K}_w(0, Z)$ is no longer a constant as soon as it is computed for a layer of variable thickness. When Z increases, the remnant light tends to become monochromatic, with the irradiance maximum centered on the minimum of K_w , and the averaged value $\bar{K}_w(0, Z)$ decreases accordingly (see Figure 4; $E_0(\lambda)$ is taken from Figure 8).

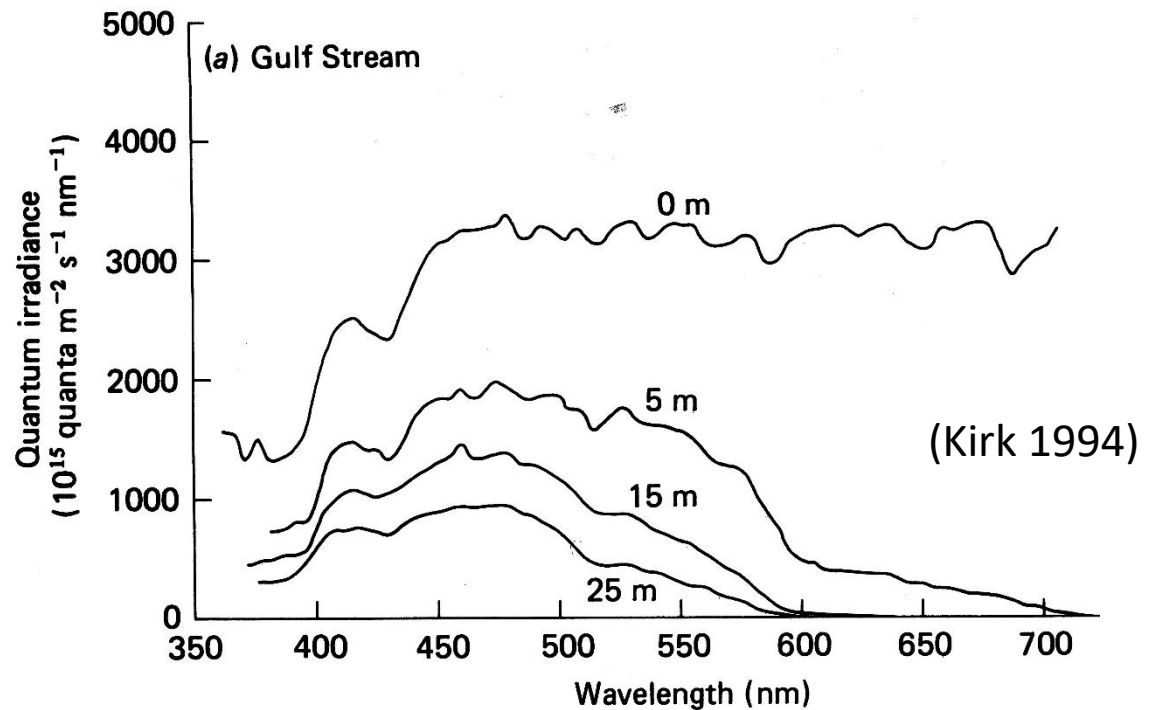
2. The constant coefficient k_c is also a doubly averaged value, over the spectrum and over the layer considered. The result of such averaging depends on the spectral composition of the underwater light and on its change with depth. Since the phytoplankton concentration depicted by C governs both

$$K_{PAR} = \frac{-1}{z} \ln \left(\frac{PAR(z)}{PAR(0)} \right)$$

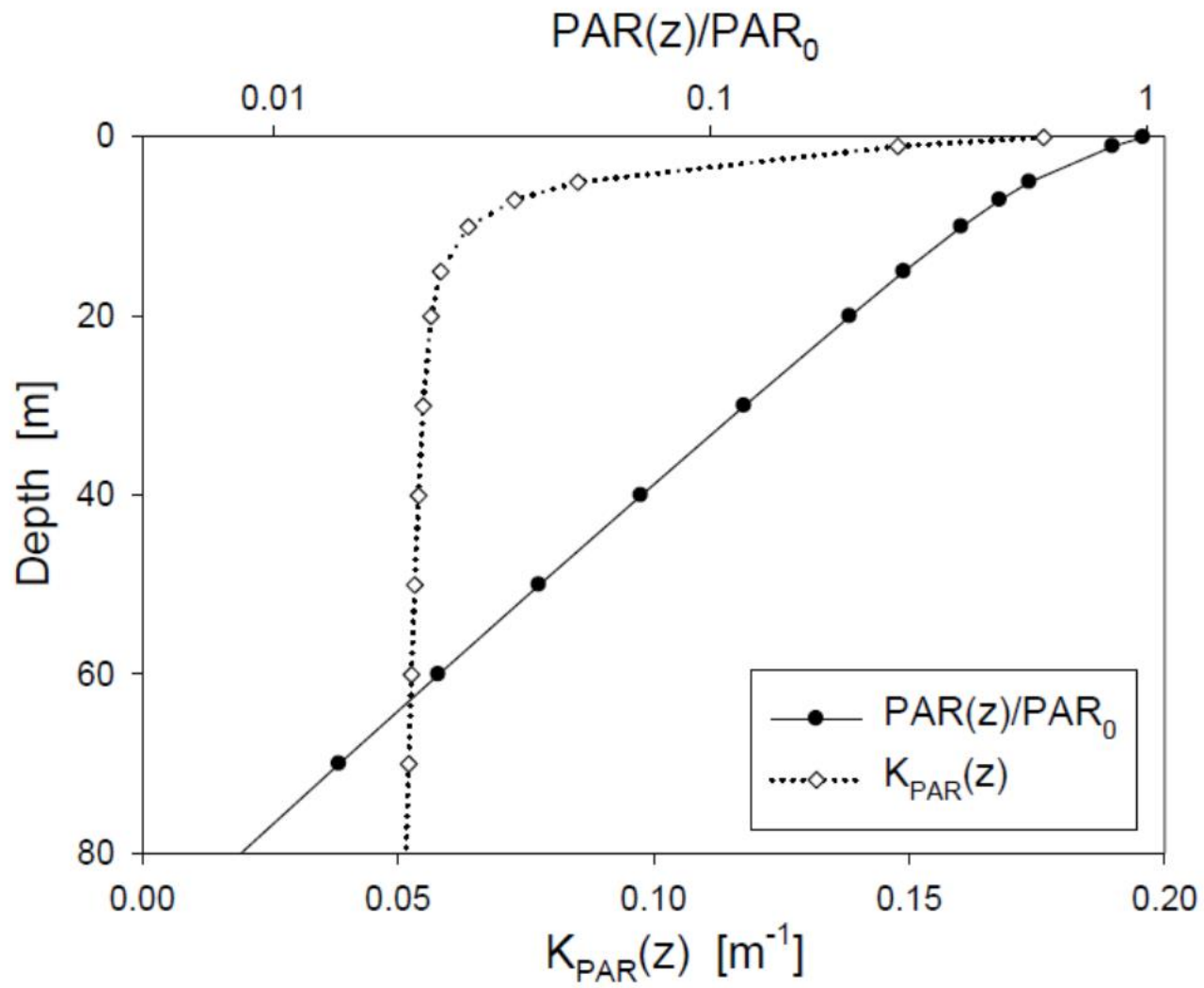
$$PAR(z) = \int_{400}^{700} E_0(\lambda, 0) e^{-K(\lambda, z)z} d\lambda$$

K_{PAR} is light-quality weighted!

Change of light with depth:



→ Light at deeper depth is associated with lower attenuation coefficient



$$PAR(z) = PAR(0) e^{-K_{par}(z) z}$$

$$K_{PAR}(z) \approx K_1 + \frac{K_2}{(1+z)^{0.5}}$$

$$K_1 = f_1(a(490), b_b(490))$$

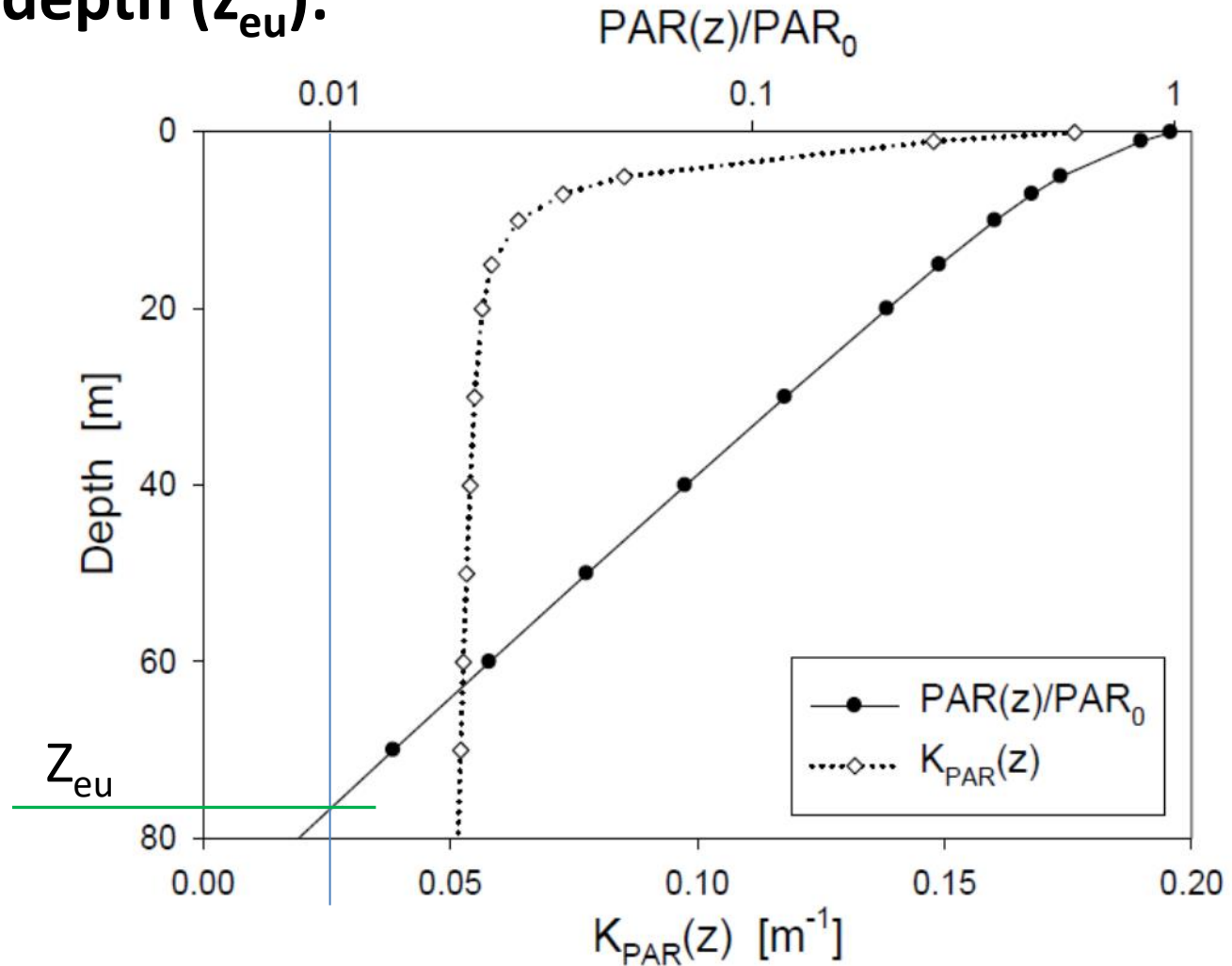
$$K_2 = f_2(a(490), b_b(490))$$

(Lee et al 2005)

Key:

K_{PAR} varies with depth, especially in the upper water column.

Euphotic depth (z_{eu}):



$$\frac{PAR(z)}{PAR(0)} = 1\%$$

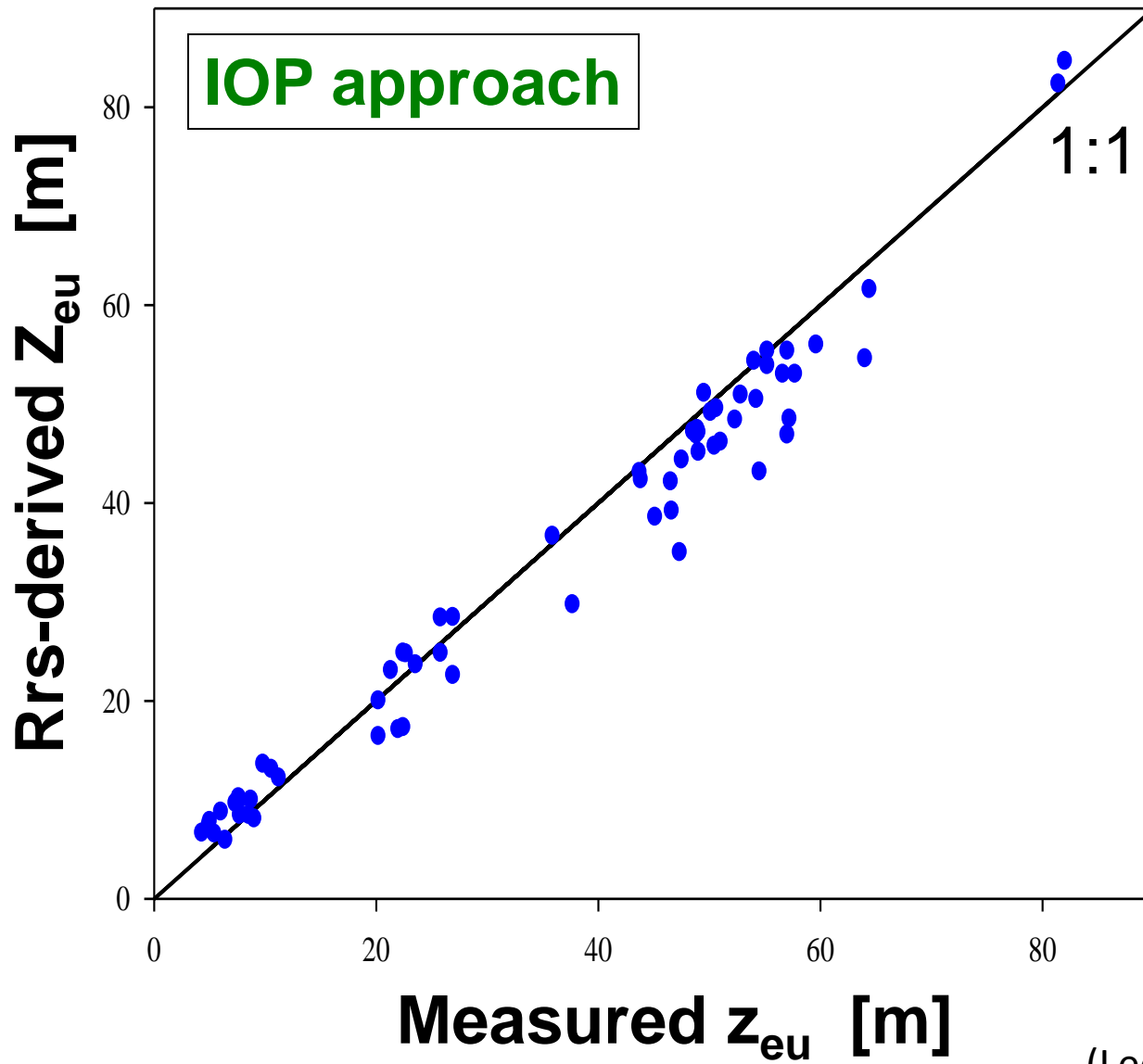
$$z_{eu} = \frac{4.6}{K_{PAR}(z_{eu})}$$



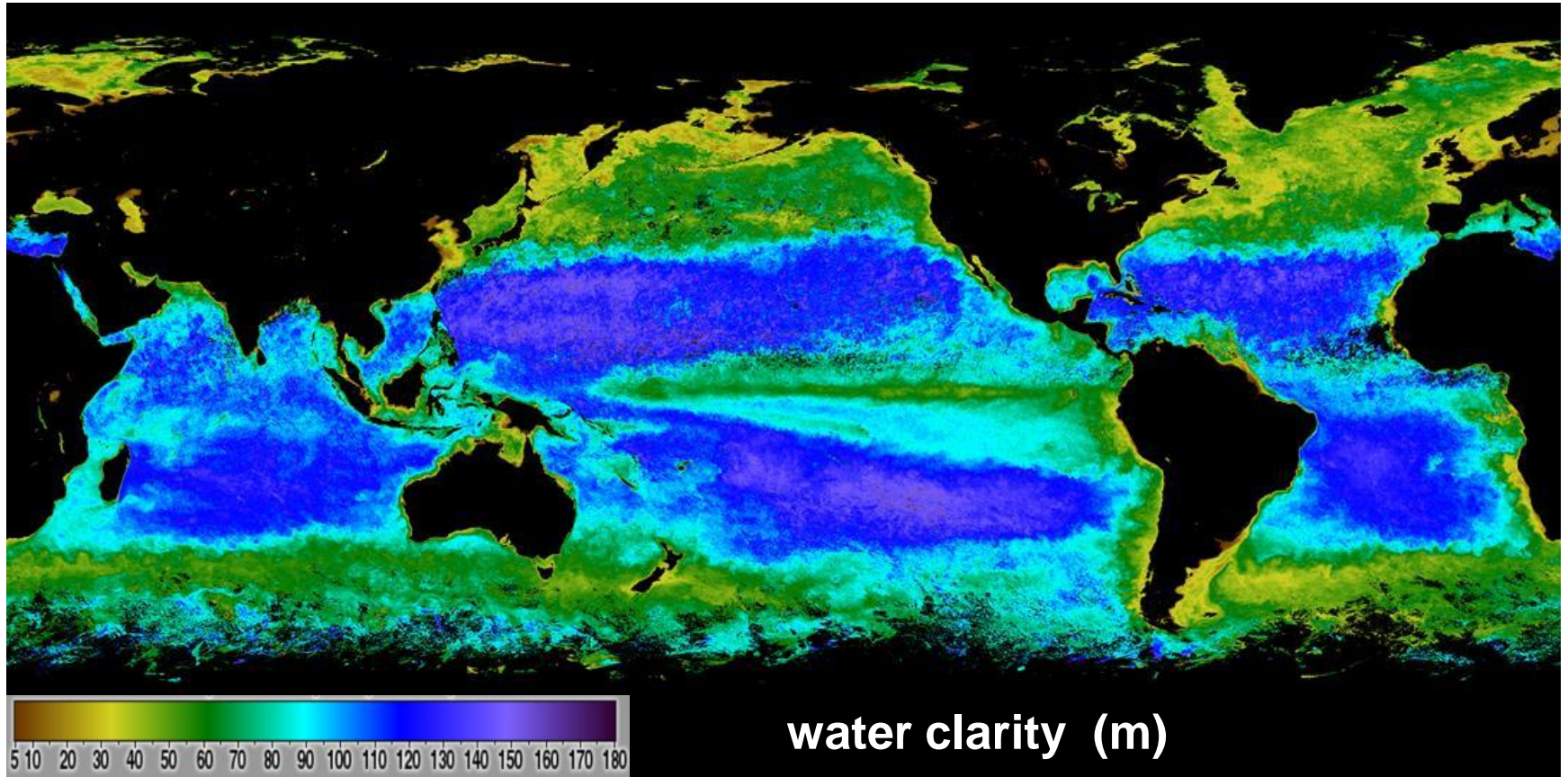
$$\left\{ K_1(a(490) \& b_b(490)) + \frac{K_2(a(490) \& b_b(490))}{(1+z_{eu})^{0.5}} \right\} z_{eu} = 4.6$$

(or 5.3 if defined as 0.5%)

$$R_{rs}(\lambda) \rightarrow a(\lambda) \& b_b(\lambda) \rightarrow K_{PAR}(z) \rightarrow z_{eu}$$



Global distribution of Z_{eu}



3. Estimation of water clarity (Secchi disk depth)

Empirical relationships for Z_{SD} derived from measurements:

Formula	Z_{SD} range (m)	Reference
$Z_{SD} = 1.7/K_{PAR}$	1.9 - 35	Poole and Atkins (1929)
$Z_{SD} = 1.44/K_{PAR}$	2 - 12	Holmes (1970)
$Z_{SD} = 1.7/K_{PAR}$	0.1 - 35	Idso (1974)
$Z_{SD} = 1.54/K_{PAR}$	6 - 46	Megard and Berman (1989)
$Z_{SD} = 1.27/K_{PAR}$	0.2 - 2.2	Gallegos et al. (1990)
$Z_{SD} = 1.86/K_{PAR}$	2.3 - 14.7	Kolengings et al. (1991)
$Z_{SD}^{1.16} = 1.48/K_{PAR}$	1.2 - 5	Montes-Hugo et al. (2005)
$Z_{SD} = 1.36/K_{PAR}$	0.1 - 42	Lugo-Fernandez (2008)
$Z_{SD}^{0.76} = 2/K_{PAR}$	0.2 - 6	Padial and Thomaz (2008)
$Z_{SD} = 1.8/K_{PAR}$	0.6 - 4.2	Bracchini et al. (2009)
$Z_{SD}^{0.85} = 1.76/K_{PAR}$	1.7 - 7.0	Ficek and Zapadka (2010)
$Z_{SD} = 1.4/K_{PAR}$	0.5 - 2.5	Gallegos et al. (2011)
$Z_{SD} = 1.37/K_{PAR}$	0.1 - 2.4	Zhang et al. (2012)

$$K_D(m^{-1}) = 0.11 + \frac{1.28}{D(m)}$$

(Lee et al 2018)

(Sathyendranath and Varadachari, 1982)

$$Z_{SD} = (1.4 \sim 1.7)/K_{PAR}$$

The theoretical relationship:

(Duntley 1952; Preisendorfer 1986; Zaneveld and Pegau 2003; Aas 2014)

$$Z_{SD} = \frac{\Gamma}{K_d + c}$$

$c \gg K_d$

$$\Gamma = \ln\left(\frac{C_i}{C_t}\right)$$

(~5 – 10)

$$C_i = \frac{r_T - r_B}{r_B}$$

K_d : Diffuse attenuation coefficient

c : Beam attenuation coefficient

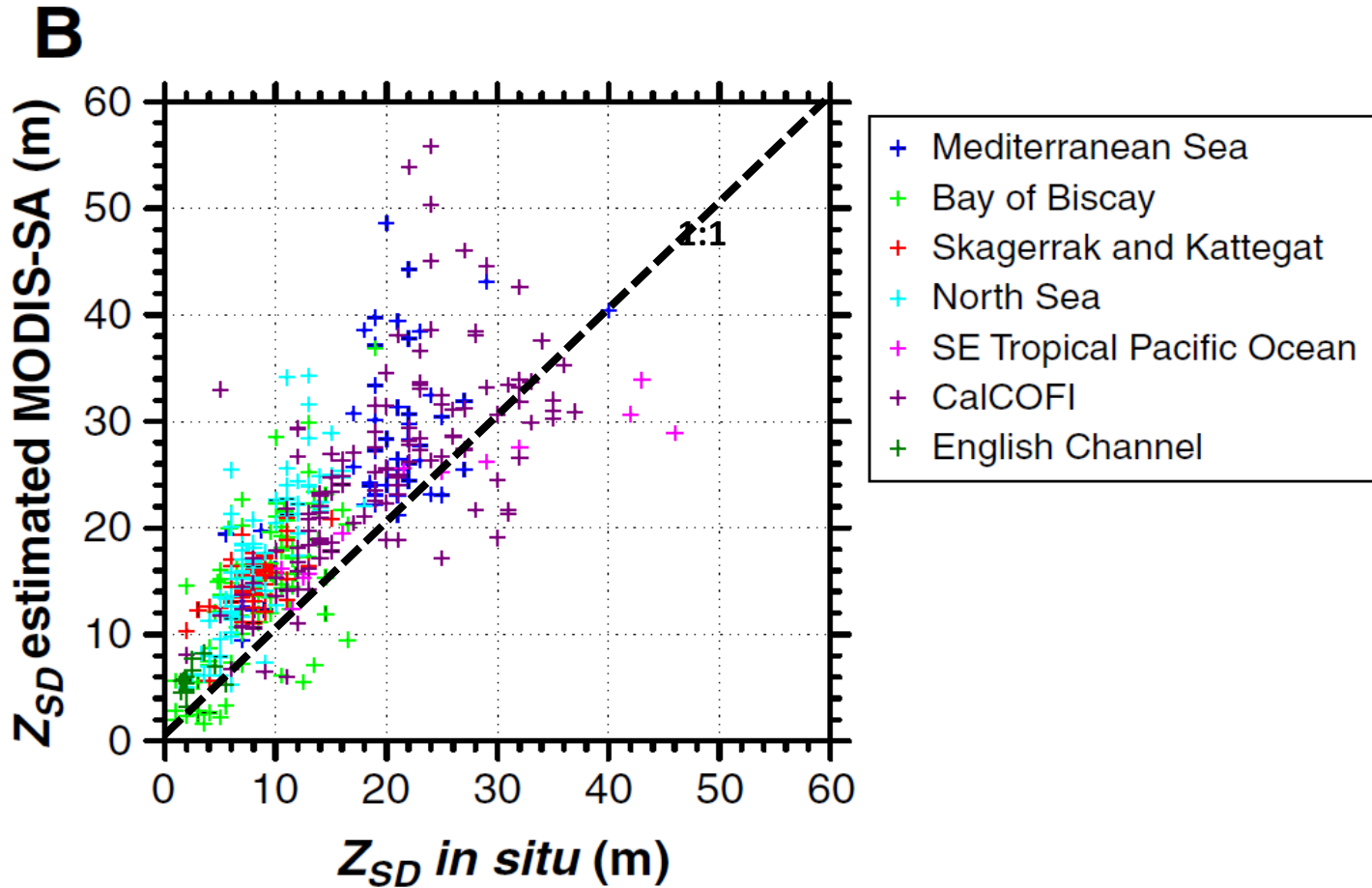
C_i : Inherent contrast

C_t : Contrast threshold of human eye; ~2%

$$Z_{SD} = (1.4-1.7)/K_{PAR}$$

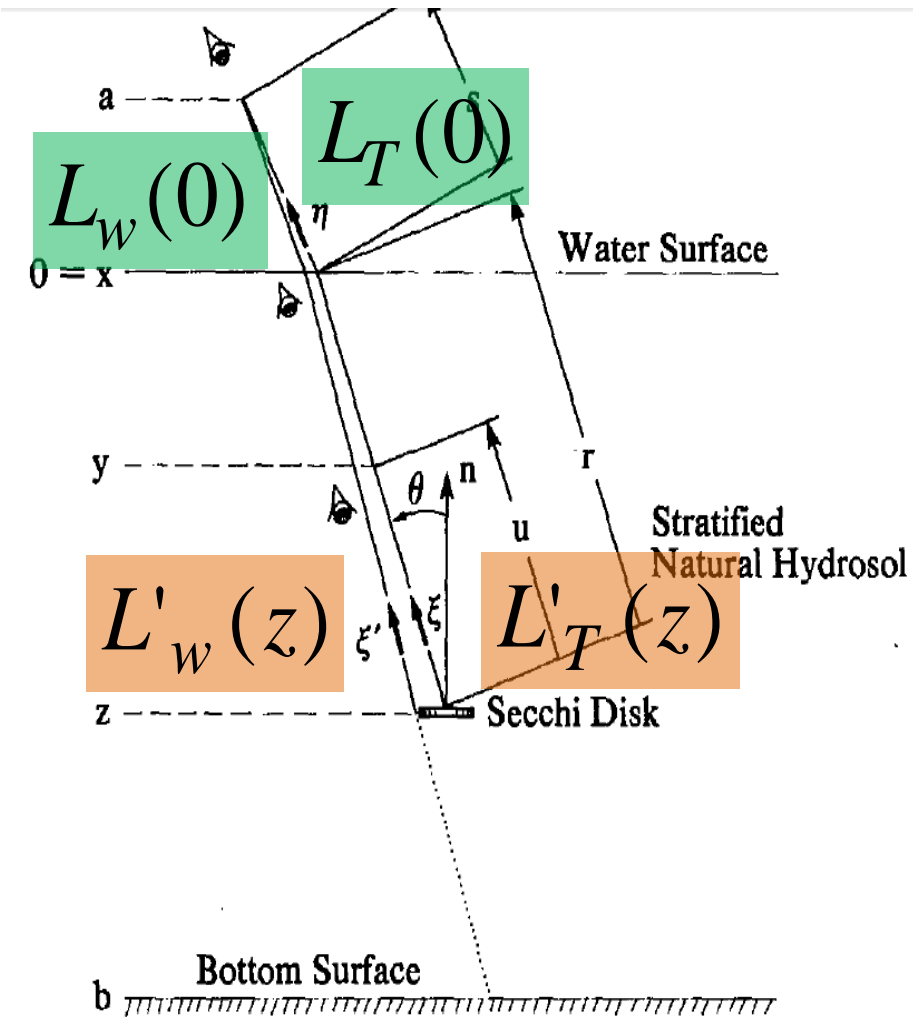
Theory and observation do not match.

Results based on classical theory



(Doron et al 2011)

Where the c comes from?

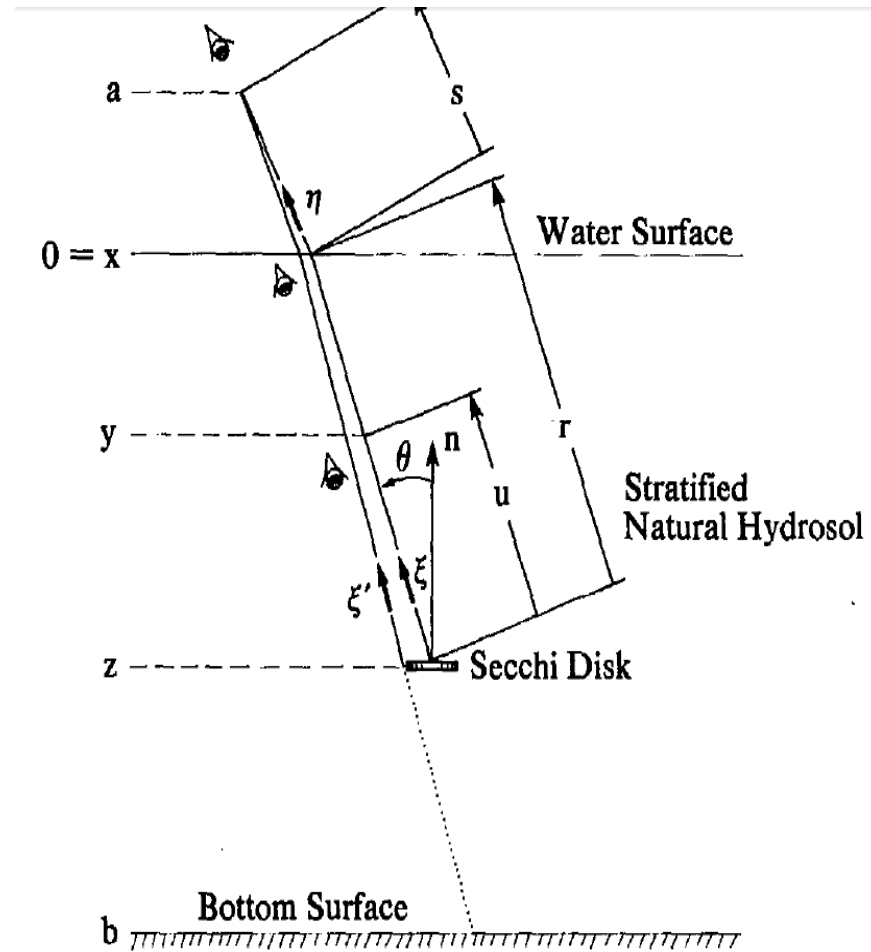


Geometry of the Secchi Disk Sighting

(Preisendorfer, 1986)

$$d \frac{L_T(z, \xi)}{dz} = -c L_T(z, \xi) + \int_{4\pi} L'_T(z) \beta d\omega$$

$$d \frac{L_w(z, \xi')}{dz} = -c L_w(z, \xi') + \int_{4\pi} L'_w(z) \beta d\omega$$



Assume:

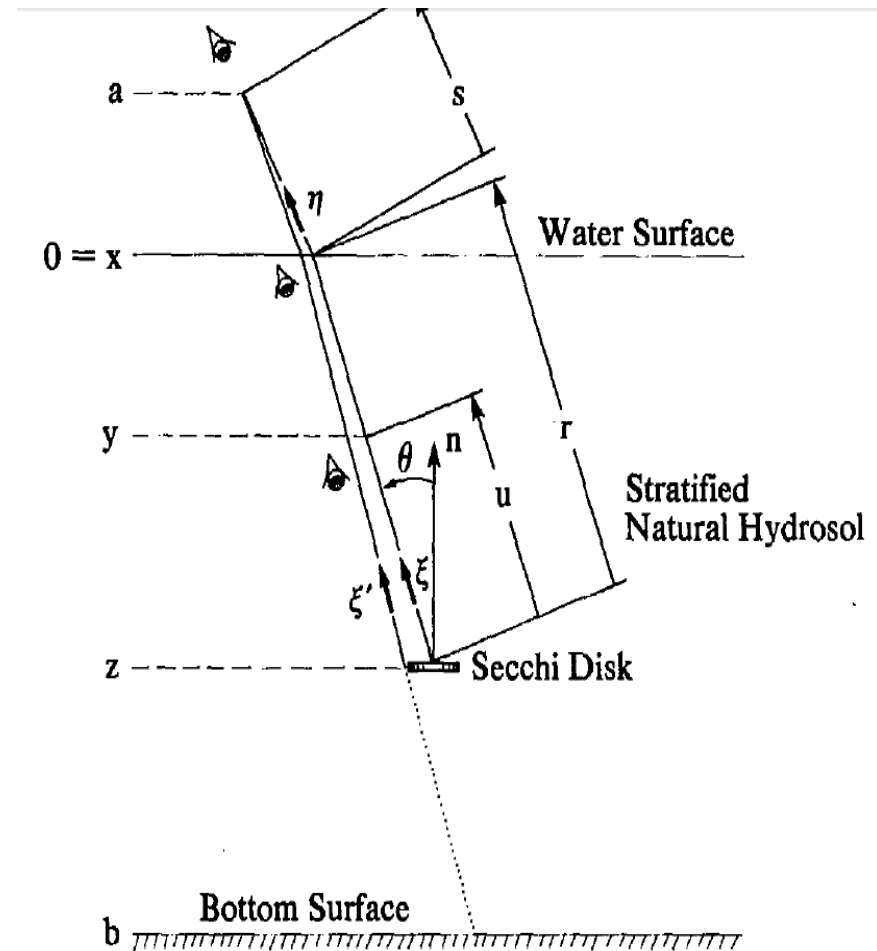
$$\int L'_T(z) \beta dw = \int L'_w(z) \beta dw$$

$$d \frac{L_T(z, \xi)}{dz} = -c L_T(z, \xi) + \int_{4\pi} L'_T(z) \beta d\omega$$

$$d \frac{L_w(z, \xi')}{dz} = -c L_w(z, \xi') + \int_{4\pi} L'_w(z) \beta d\omega$$

$$d \frac{L_T(z) - L_w(z)}{dz} = -c(L_T(z) - L_w(z))$$

$$Z_{SD} = \frac{1}{(c+K)} \ln \left(\frac{C_i}{C_t} \right) = \frac{\Gamma}{(c+K)}$$



Geometry of the Secchi Disk Sighting

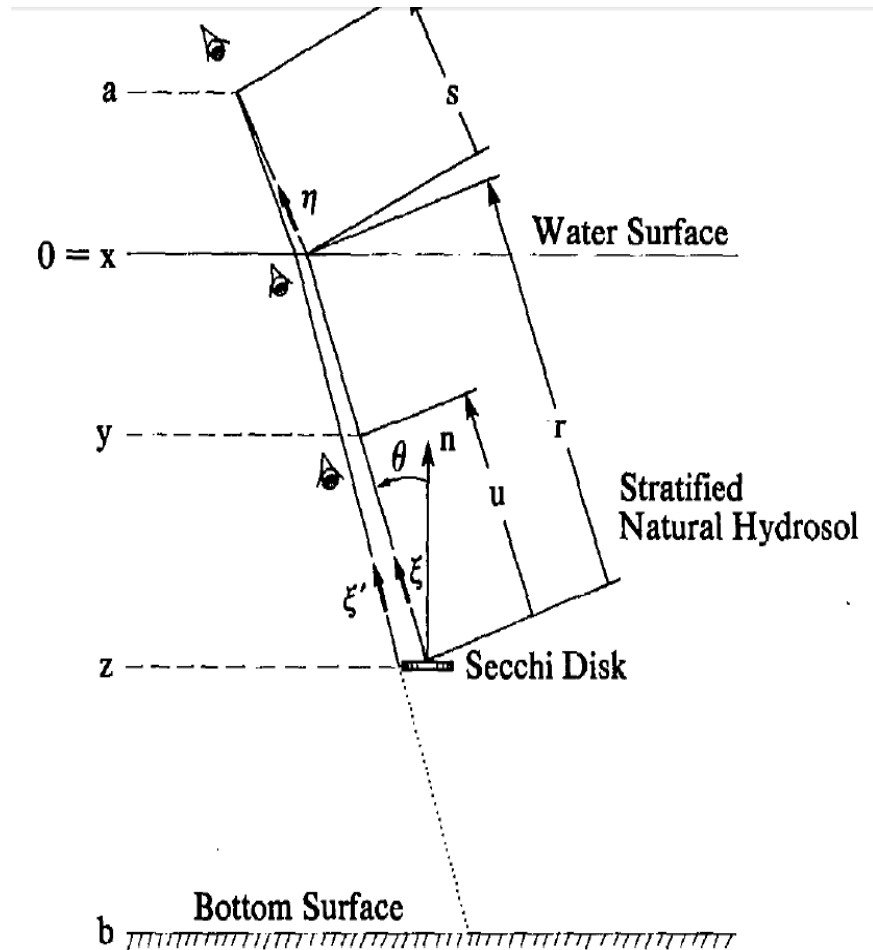
$$\int L'_T(z) \beta dw = \int L'_w(z) \beta dw \quad ??$$

Point source:

$$\int L'_T(z) \beta dw = \int L'_w(z) \beta dw$$

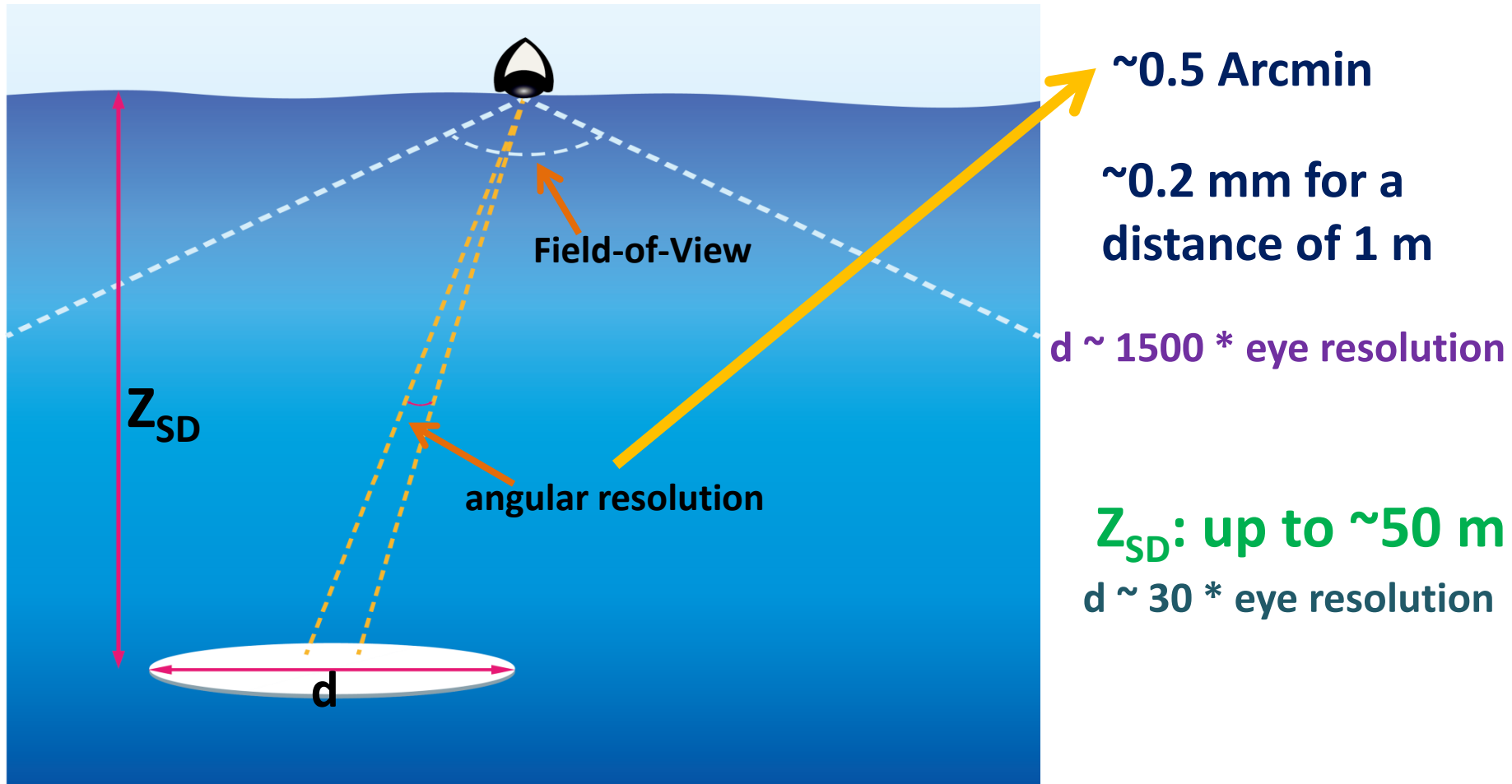
Does this assumption hold for observing a Secchi disk?

Is a Secchi disk a point to our eye?



Geometry of the Secchi Disk Sighting

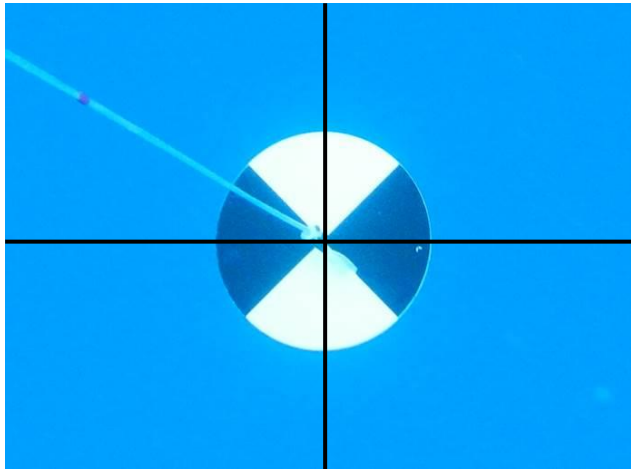
Secchi disk vs the resolution of eye “sensor”



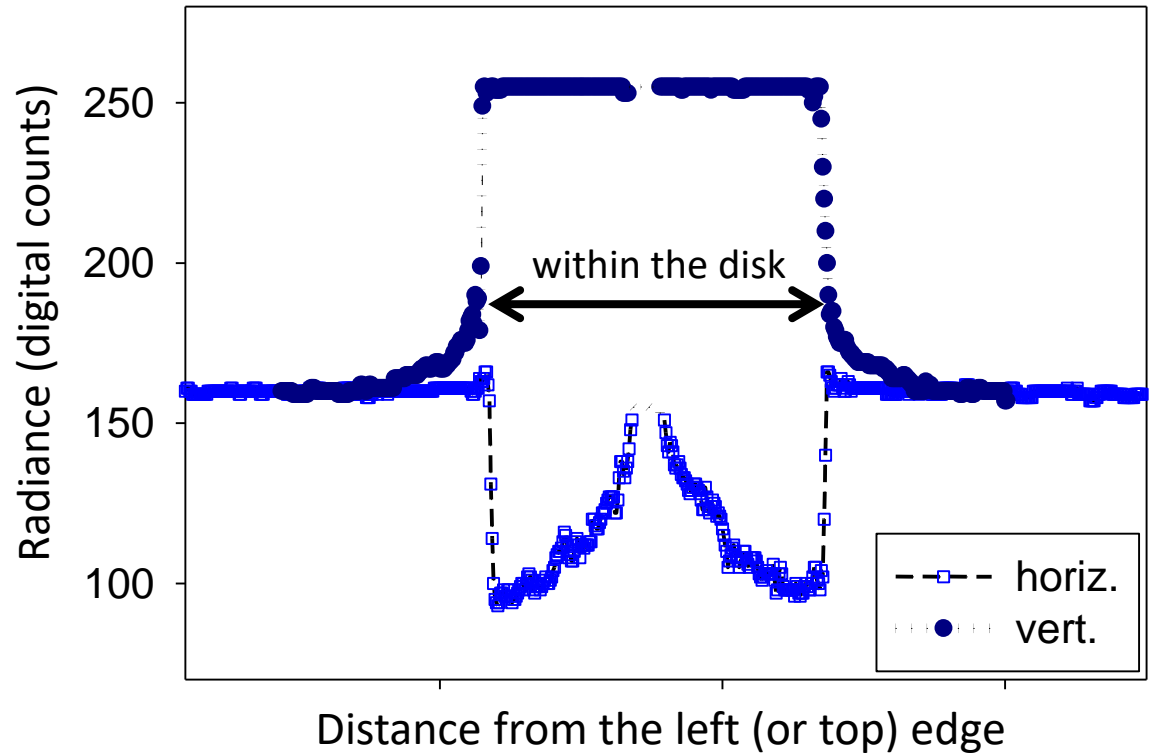
For a radiance sensor with a 5° resolution, the equivalent target is ~ 120-m wide when viewed 1 m away.

➡ A Secchi disk is **NOT** a point source for human eyes.

Spatial variation of radiance around a Secchi disk:



(Lee et al 2015)



$$\int L'_T(z) \beta dw \neq \int L'_w(z) \beta dw$$

$$d \frac{L_T(z, \xi)}{dz} = -c L_T(z, \xi) + \int_{4\pi} L'_T(z) \beta d\omega$$

$$d \frac{L_w(z, \xi')}{dz} = -c L_w(z, \xi') + \int_{4\pi} L'_w(z) \beta d\omega$$

$$\int L'_T(z) \beta d\omega \neq \int L'_w(z) \beta d\omega$$



$$d \frac{L_T(z) - L_w(z)}{dz} \neq -c(L_T(z) - L_w(z))$$



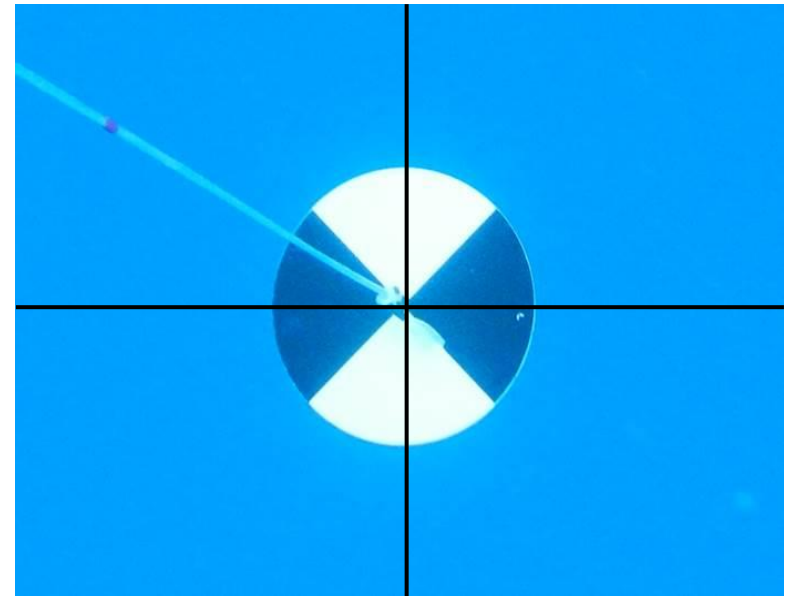
$$Z_{SD} \neq \frac{\Gamma}{K + c}$$

Quantification of contrast:

$$C_i = \frac{r_T - r_B}{r_B}$$

r_T : reflectance of target

r_B : reflectance of background



$r_B ?$

Contrast for detection:

$$L^C = L_T - L_B$$

d ~ 50 * the resolution of “eye sensor”



A Secchi disk is a sinking “bottom” to human eye

- Use the most transparent (tr) band to sight the disk
- Following “brightness consistency”

Radiative transfer of shallow bottom:

$$L_T^{tr}(0^-) = r_w^{tr} \times E_d^{tr}(0^-) \left(1 - e^{-(K_d^{tr} + K_L^{tr})z}\right) + r_T \times E_d^{tr}(0^-) e^{-(K_d^{tr} + K_L^{tr})z}$$

Adjacent water:

$$L_w^{tr}(0^-) = r_w^{tr} E_d^{tr}(0^-)$$

$K_{d,L}^{tr}$: attenuation coefficient in the transparent window

Contrast in radiance:

$$L^C = L_T^{tr}(0^-) - L_w^{tr}(0^-) = r_w^{tr} \times E_d^{tr}(0^-) \left(-e^{-(K_d^{tr} + K_L^{tr})z}\right) + r_T \times E_d^{tr}(0^-) e^{-(K_d^{tr} + K_L^{tr})z}$$

Eye-adapted Contrast:

$$C_a^r = \frac{L_T^{tr}(0^-) - L_w^{tr}(0^-)}{E_d^{tr}(0^-)}$$

$$L_T^{tr}(0^-) - L_w^{tr}(0^-) = r_w^{tr} \times E_d^{tr}(0^-) \left(-e^{-(K_d^{tr} + K_L^{tr})z} \right) + r_T \times E_d^{tr}(0^-) e^{-(K_d^{tr} + K_L^{tr})z}$$



$$C_a^r = (r_T - r_w^{tr}) e^{-(K_d^{tr} + K_L^{tr})z}$$

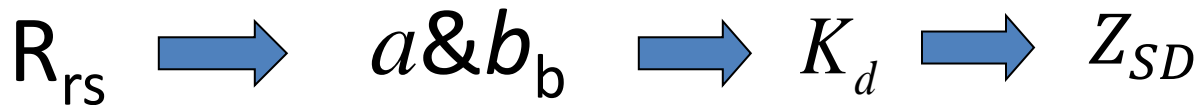
$$C_a^r = C_t^r \longrightarrow Z_{SD}$$

C_t^r : Contrast threshold in reflectance

New theoretical relationship for Z_{SD} :

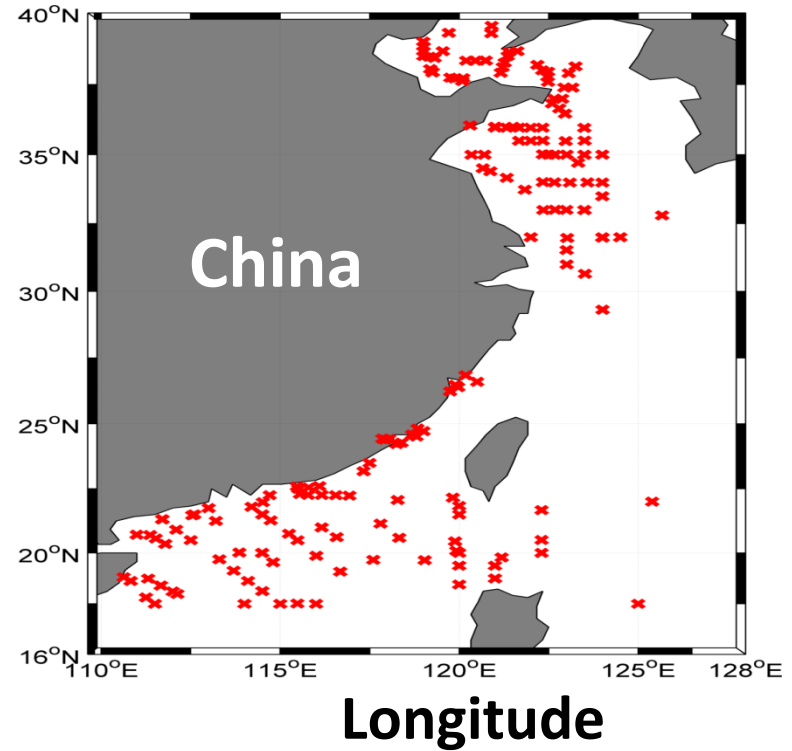
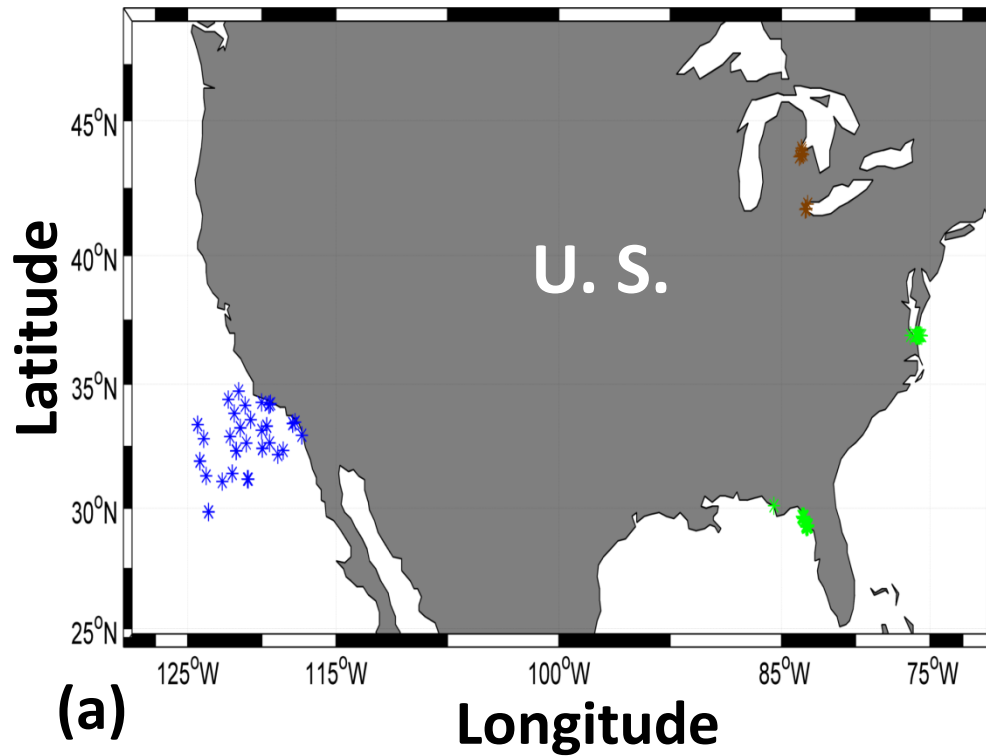
$$Z_{SD} = \frac{1}{K_d^{tr} + K_L^{tr}} \ln \left(\frac{1}{C_t^r} (r_T - r_w^{tr}) \right)$$

$$Z_{SD} \approx \frac{1}{K_d^{tr}} \approx \frac{1.4}{K_{PAR}}$$

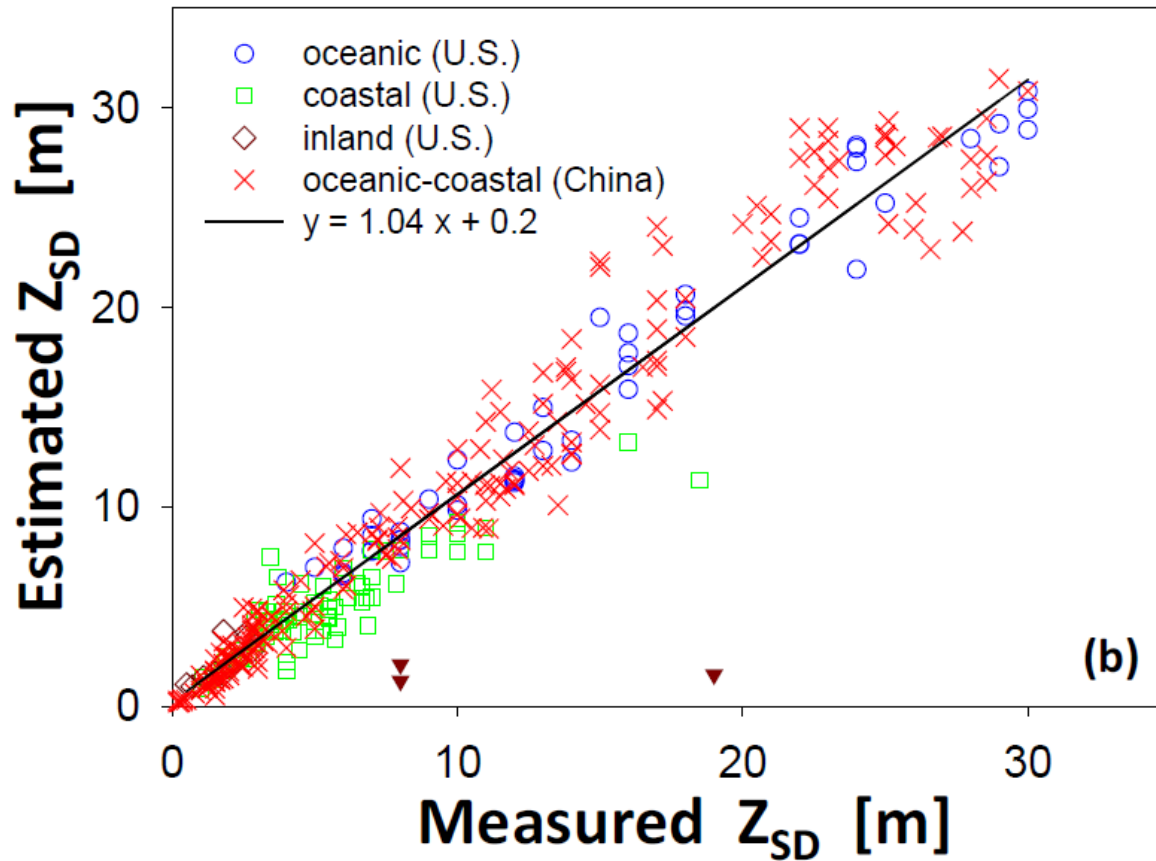


(Lee et al 2015)

Verification of the new Secchi disk theory

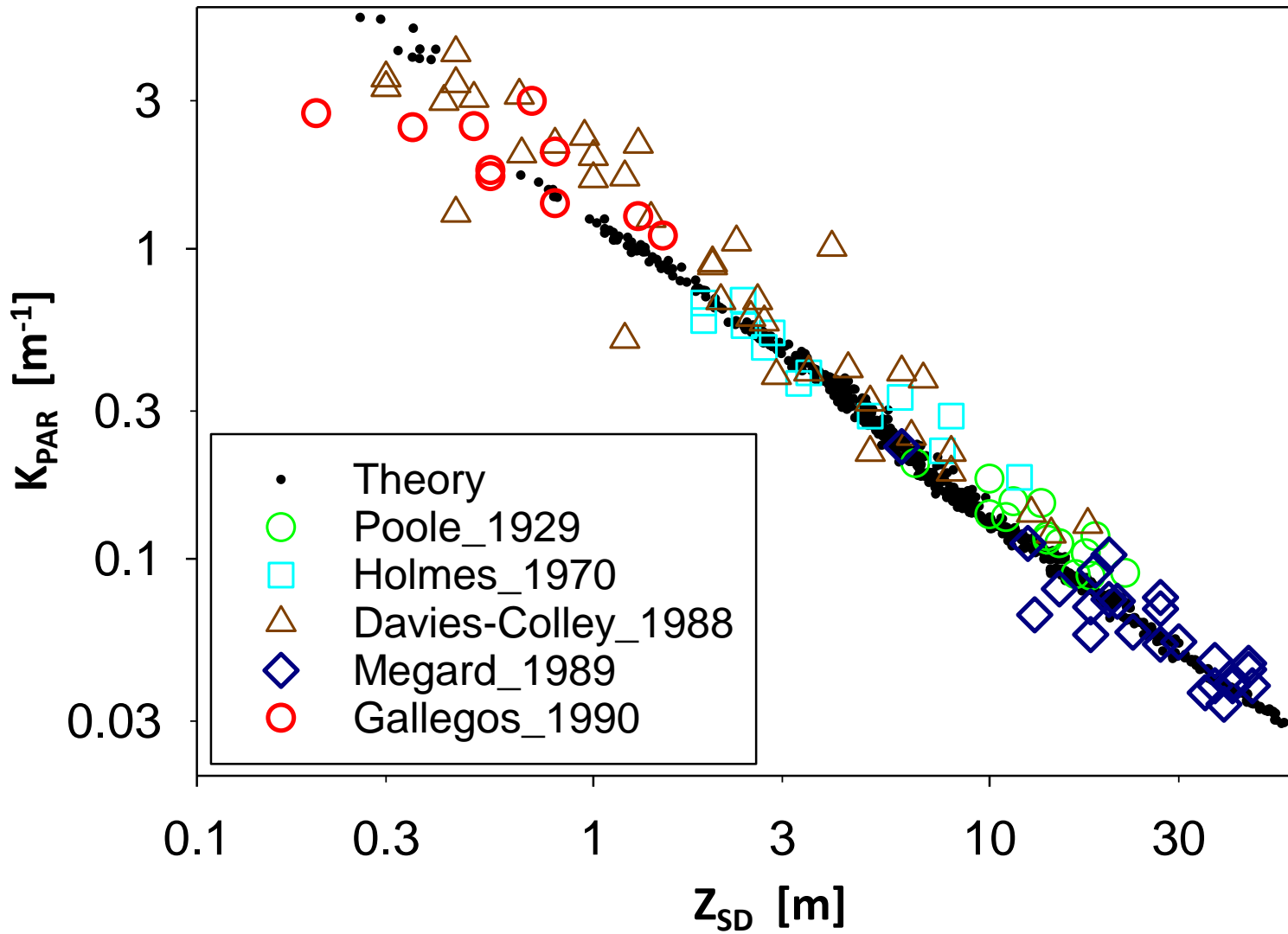


Verification of the new Secchi disk theory



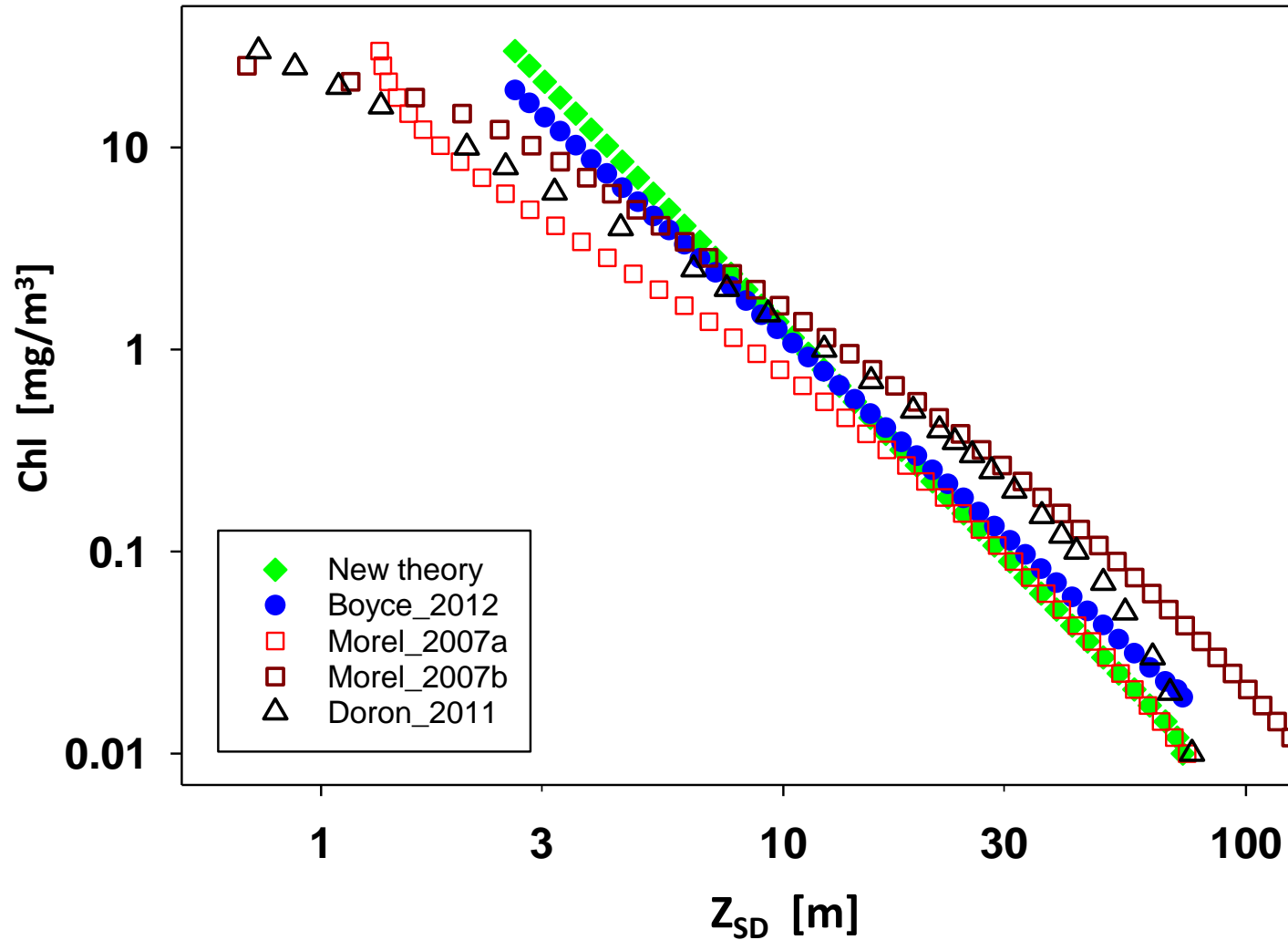
(Lee et al 2015)

With K_d^{tr} as the minimum K_d among 410, 440, 490, 530, and 550 nm



(Lee et al 2018)

Z_{SD} vs Chl for “Case-1” waters



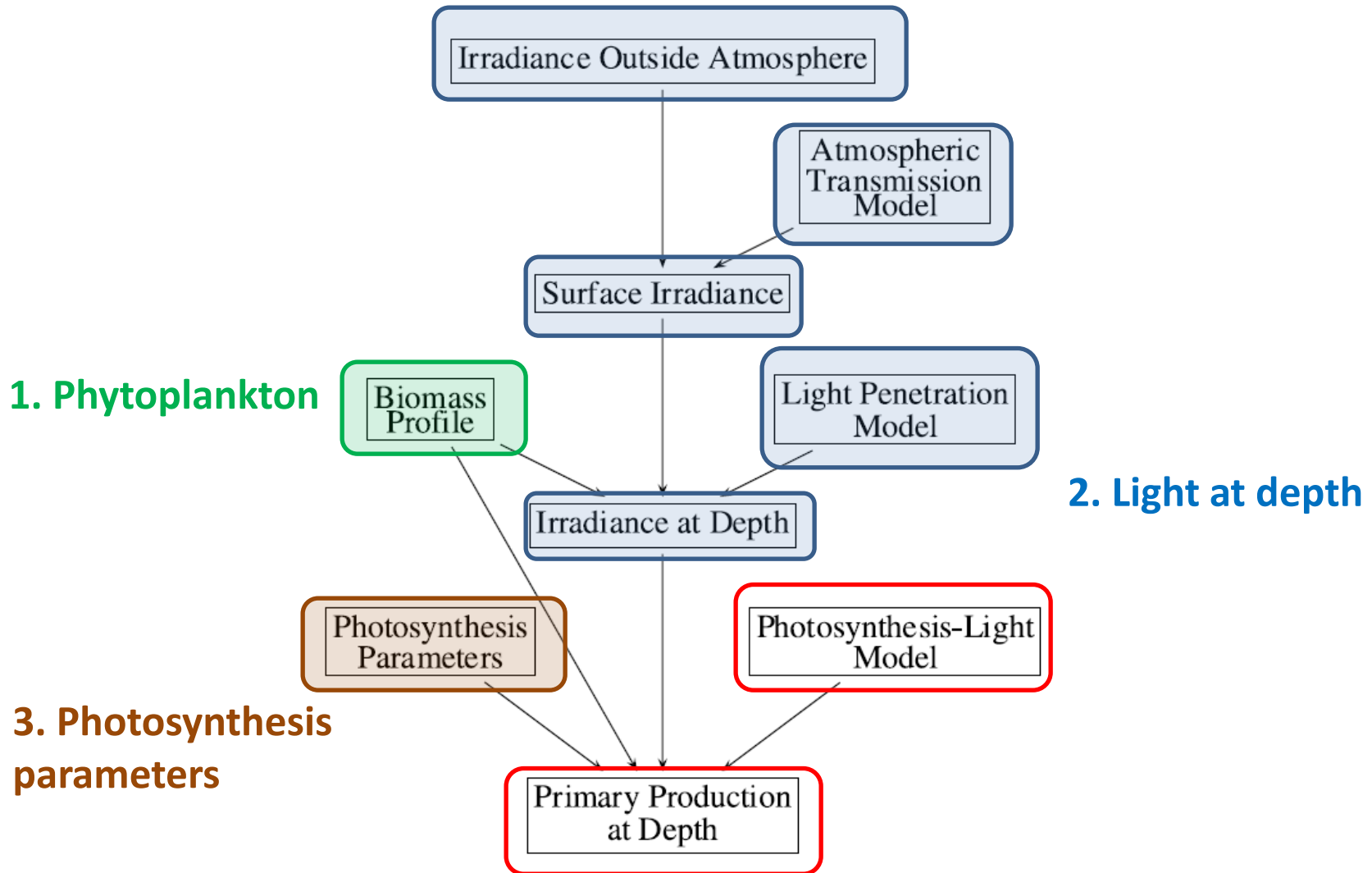
(Lee et al 2018)

4. Estimation of primary production

“One of the principal applications of satellite ocean color data is to derive **net primary production** (NPP).” --- McClain (Annu. Rev. Mar. Sci., 2009)

“On a global scale, marine phytoplankton consume fifty thousand million tones of carbon every year in a process referred to as **primary production.**” --
IOCCG Report #2

Components for PP estimation:



(from Platt and Sathyendranath)

Traditionally Chl is used to represent phytoplankton

I. Wavelength-resolved models (WRMs)

$$\sum PP = \int_{\lambda=400}^{700} \int_{t=\text{sunrise}}^{\text{sunset}} \int_{z=0}^{Z_{\text{eu}}} \Phi(\lambda, t, z) \times \text{PAR}(\lambda, t, z) \times a^*(\lambda, z) \times \text{Chl}(z) \, d\lambda \, dt \, dz - R$$

II. Wavelength-integrated models (WIMs)

$$\sum PP = \int_{t=\text{sunrise}}^{\text{sunset}} \int_{z=0}^{Z_{\text{eu}}} \varphi(t, z) \times \text{PAR}(t, z) \times \text{Chl}(z) \, dt \, dz - R$$

III. Time-integrated models (TIMs)

$$\sum PP = \int_{z=0}^{Z_{\text{eu}}} P^b(z) \times \text{PAR}(z) \times DL \times \text{Chl}(z) \, dz$$

IV. Depth-integrated models (DIMs)

$$\sum PP = P^b_{\text{opt}} \times f[\text{PAR}(0)] \times DL \times \text{Chl} \times Z_{\text{eu}}$$

(Behrenfeld and Falkowski, 1997)

I. Wavelength-resolved models (WRMs)

$$\sum PP = \int_{\lambda=400}^{700} \int_{t=\text{sunrise}}^{\text{sunset}} \int_{z=0}^{z_{eu}} \Phi(\lambda, t, z) \times \text{PAR}(\lambda, t, z) \times a^*(\lambda, z) \times \text{Chl}(z) d\lambda dt dz - R$$

Quantum yield of photosynthesis

$$a^*(\lambda) = \frac{a_{ph}(\lambda)}{Chl}$$

a_{ph} : Absorption coefficient of phytoplankton

II. Wavelength-integrated models (WIMs)

$$\sum PP = \int_{t=\text{sunrise}}^{\text{sunset}} \int_{z=0}^{z_{eu}} \varphi(t, z) \times \text{PAR}(t, z) \times \text{Chl}(z) dt dz - R$$

Centered on Chl

I. Wavelength-resolved models (WRMs)

$$\sum PP = \int_{\lambda=400}^{700} \int_{t=\text{sunrise}}^{\text{sunset}} \int_{z=0}^{z_{eu}} \Phi(\lambda, t, z) \times \text{PAR}(\lambda, t, z) \times a^*(\lambda, z) \times \text{Chl}(z) d\lambda dt dz - R$$

$$\sum PP = \int \int \phi(\lambda, t, z) \times \text{PAR}(\lambda, t, z) \times a_{ph}(\lambda, z) d\lambda dt - R$$

Centered on a_{ph}

$$\sum PP = \int_{t=\text{sunrise}}^{\text{sunset}} \int_{z=0}^{Z_{\text{eu}}} \varphi(t, z) \times \text{PAR}(t, z) \times \text{Chl}(z) dt dz$$

$$\sum PP = \int \int \phi(\lambda, t, z) \times \text{PAR}(\lambda, t, z) \times a_{ph}(\lambda, z) d\lambda dt$$

Contrast in mathematics and physics of the two approaches:

φ vs ϕ :

φ involves both ϕ and a^* .

Chl vs a_{ph} :

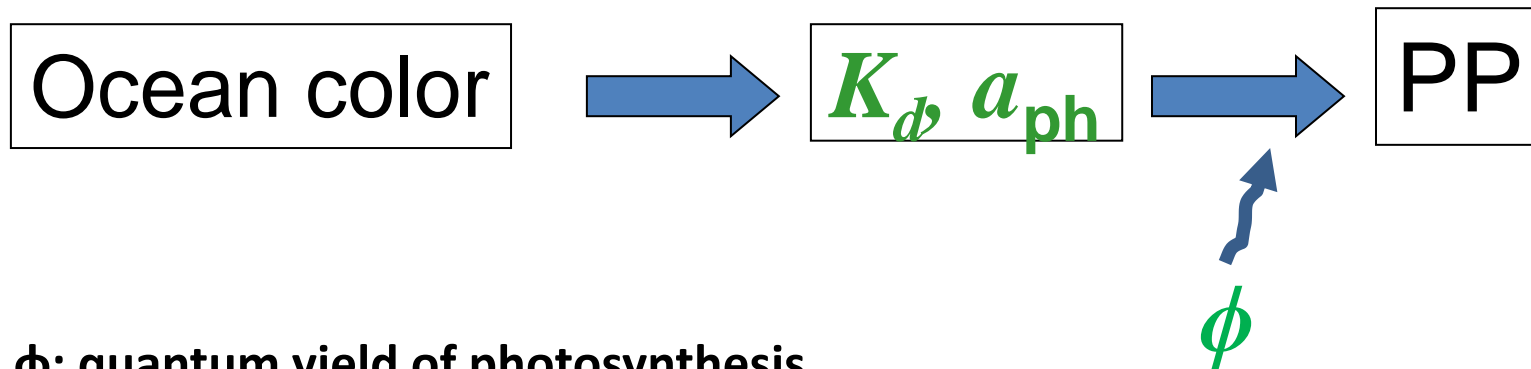
Chl is a biological property; **could not be** directly obtained from OC remote sensing.

a_{ph} is an optical property; ocean color measures optical property.

Absorption based model for PP

$$PP(z) = \iint \phi \times E_0(\lambda, t, z) \times a_{ph}(\lambda, z) d\lambda dt$$

A more direct representation of photosynthesis.

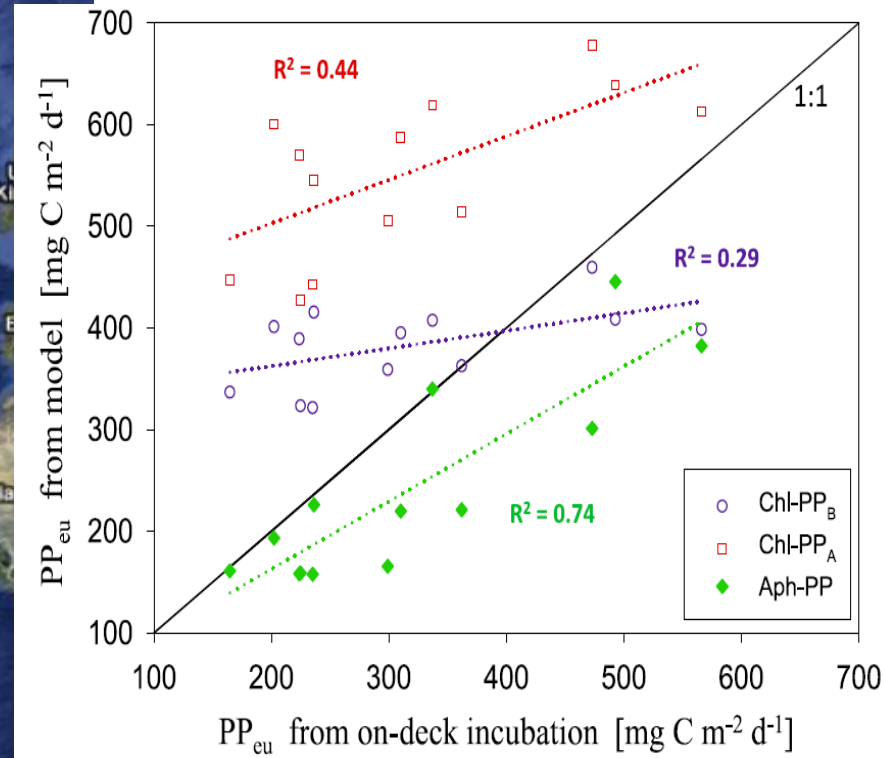
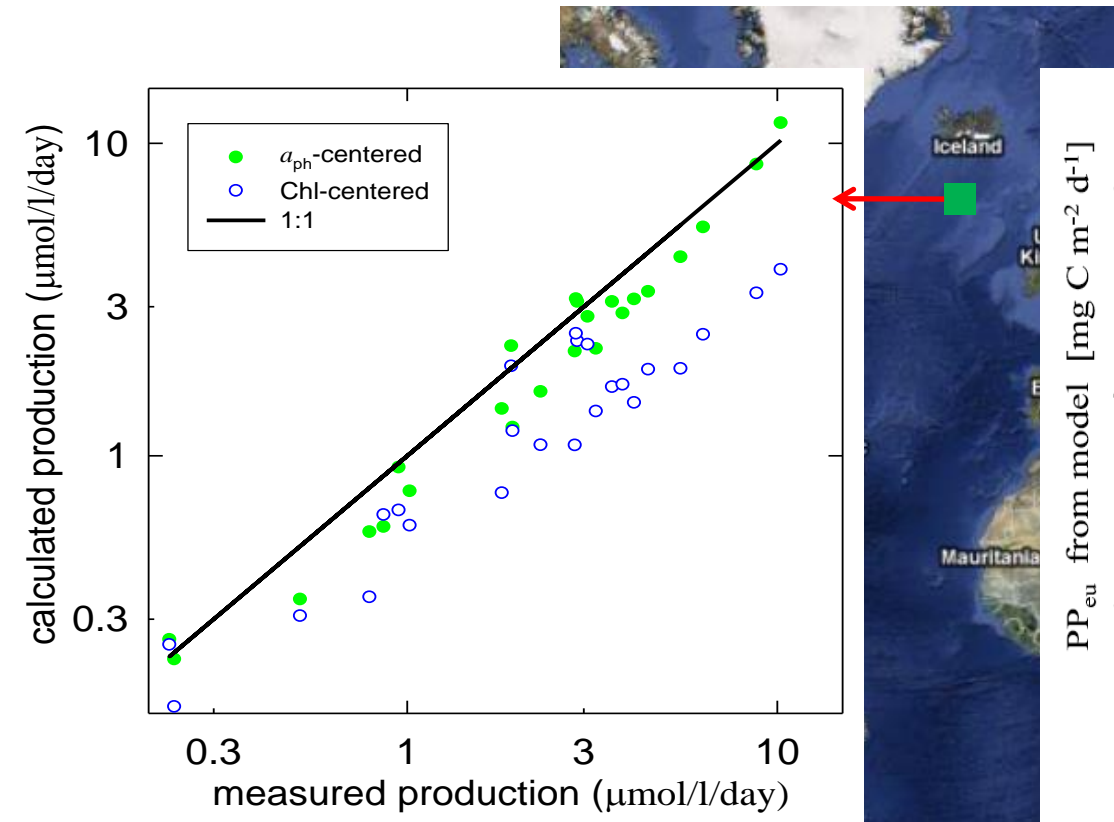


ϕ : quantum yield of photosynthesis

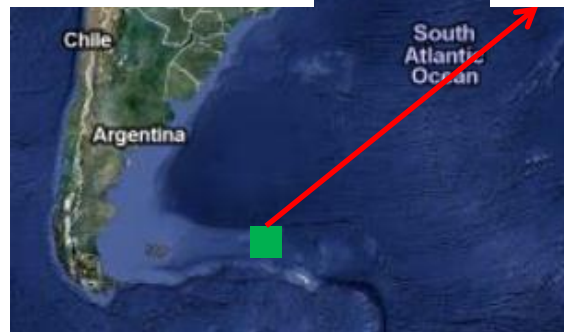
$$\phi(E_0) = \frac{\phi_m K_\phi}{K_\phi + E_0} \quad (2)$$

(Kiefer and Mitchell, 1983, L&O)

Remotely-estimated PP compared with measured PP



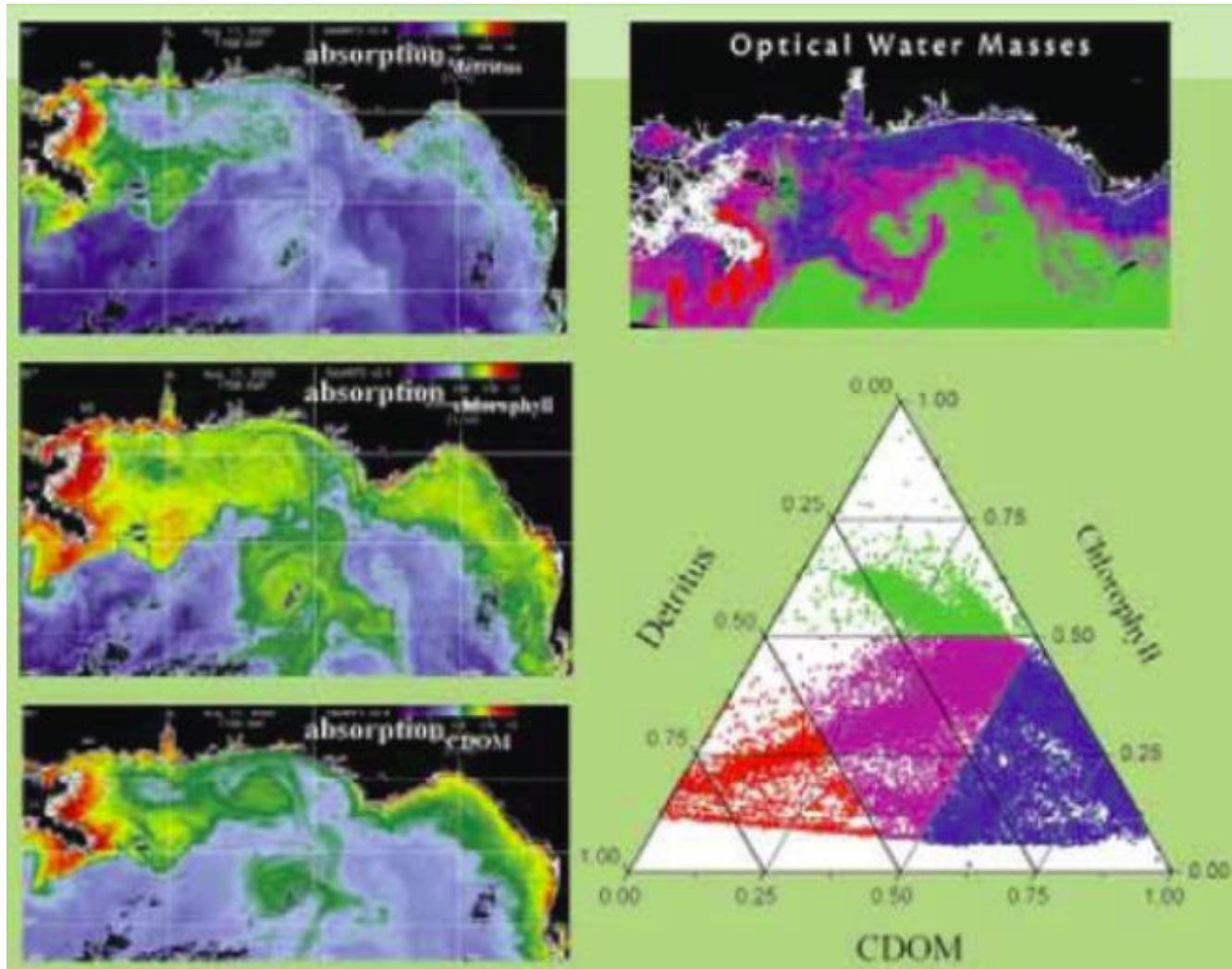
(redraw from Lee et al., Appl. Opt., 1996)



(Lee et al., JGR, 2011)

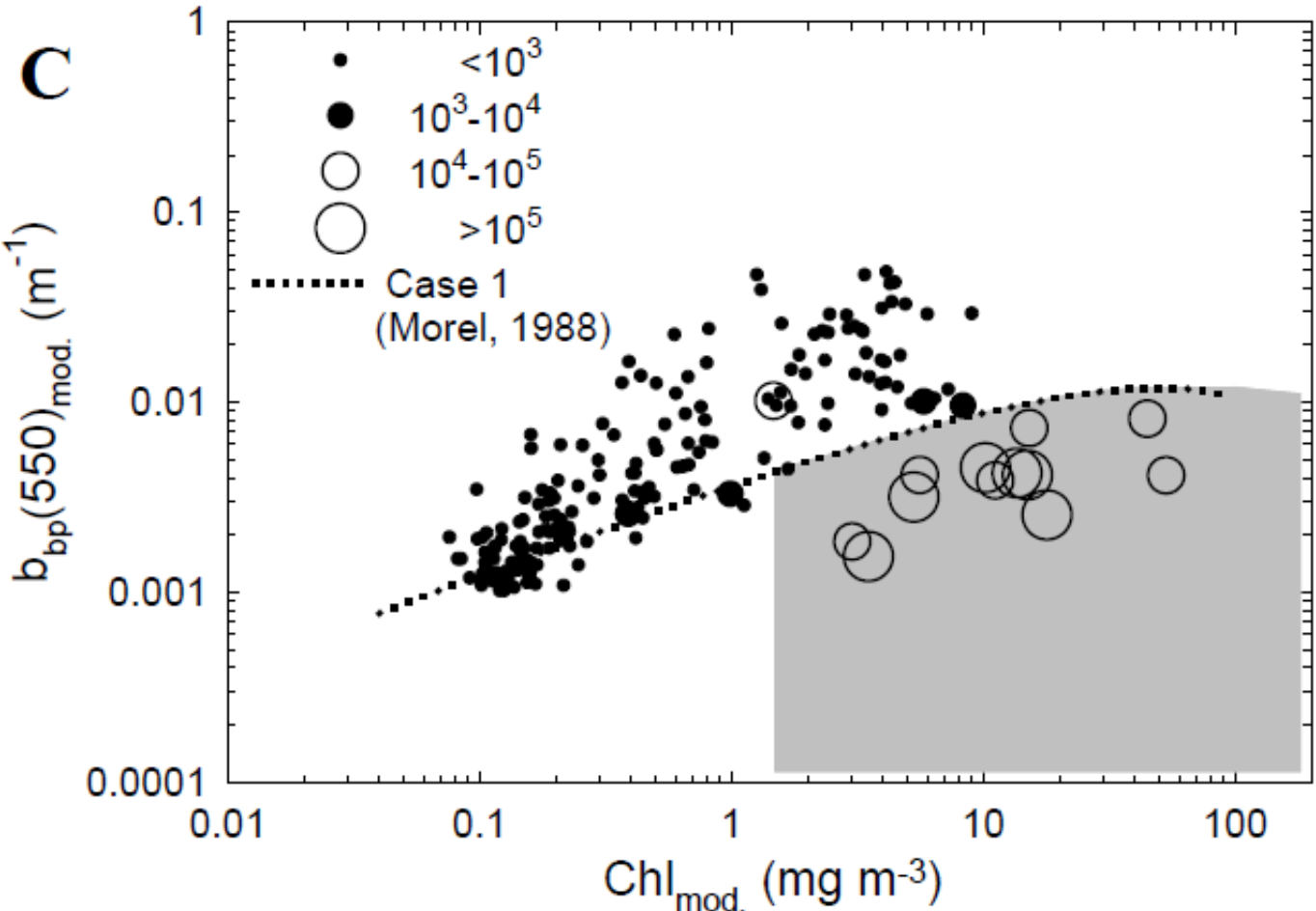
5. A few other examples

5a. Water mass classification



(Arnone et al 2004)

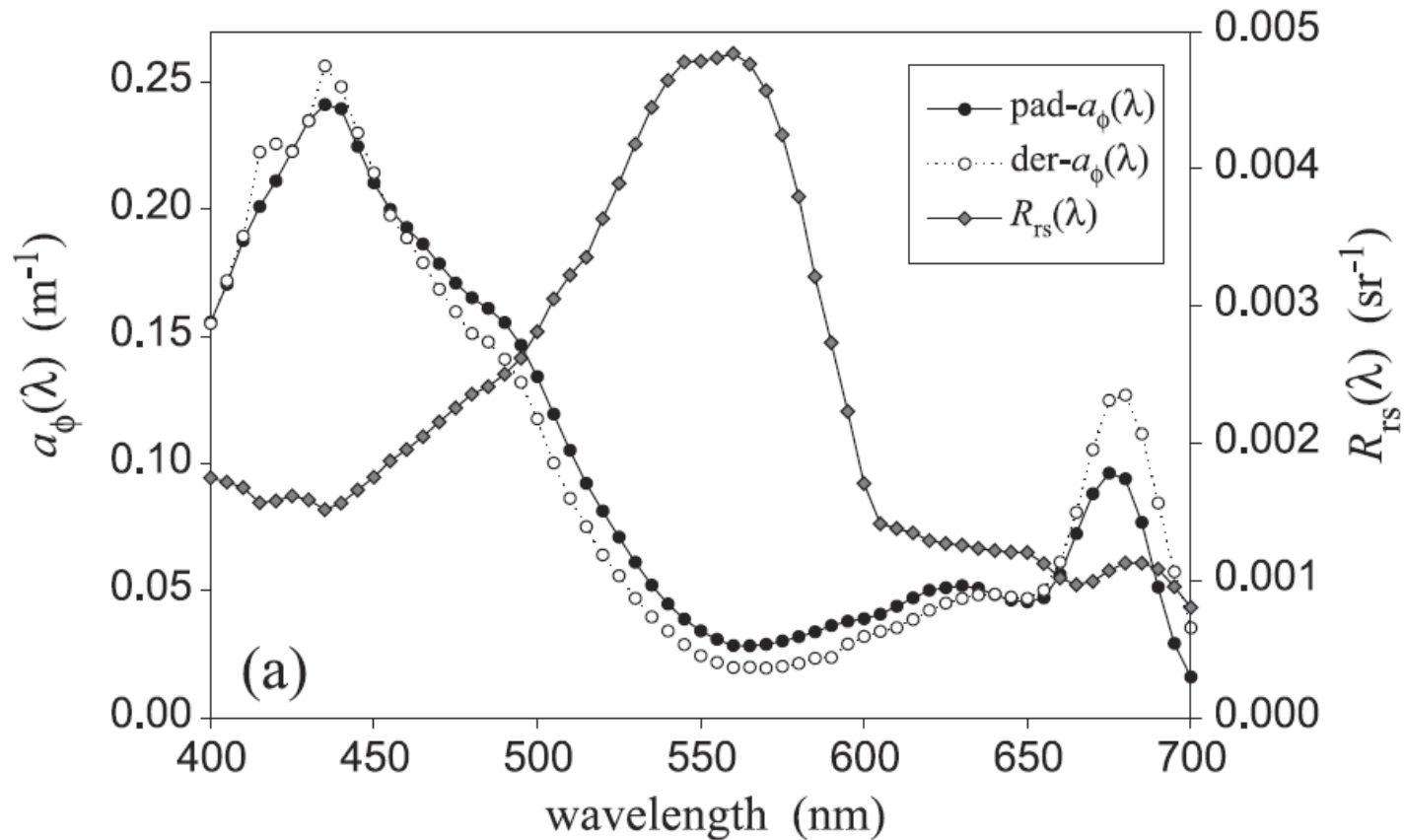
5b. HAB identification-1



(Carnizzaro et al 2008)

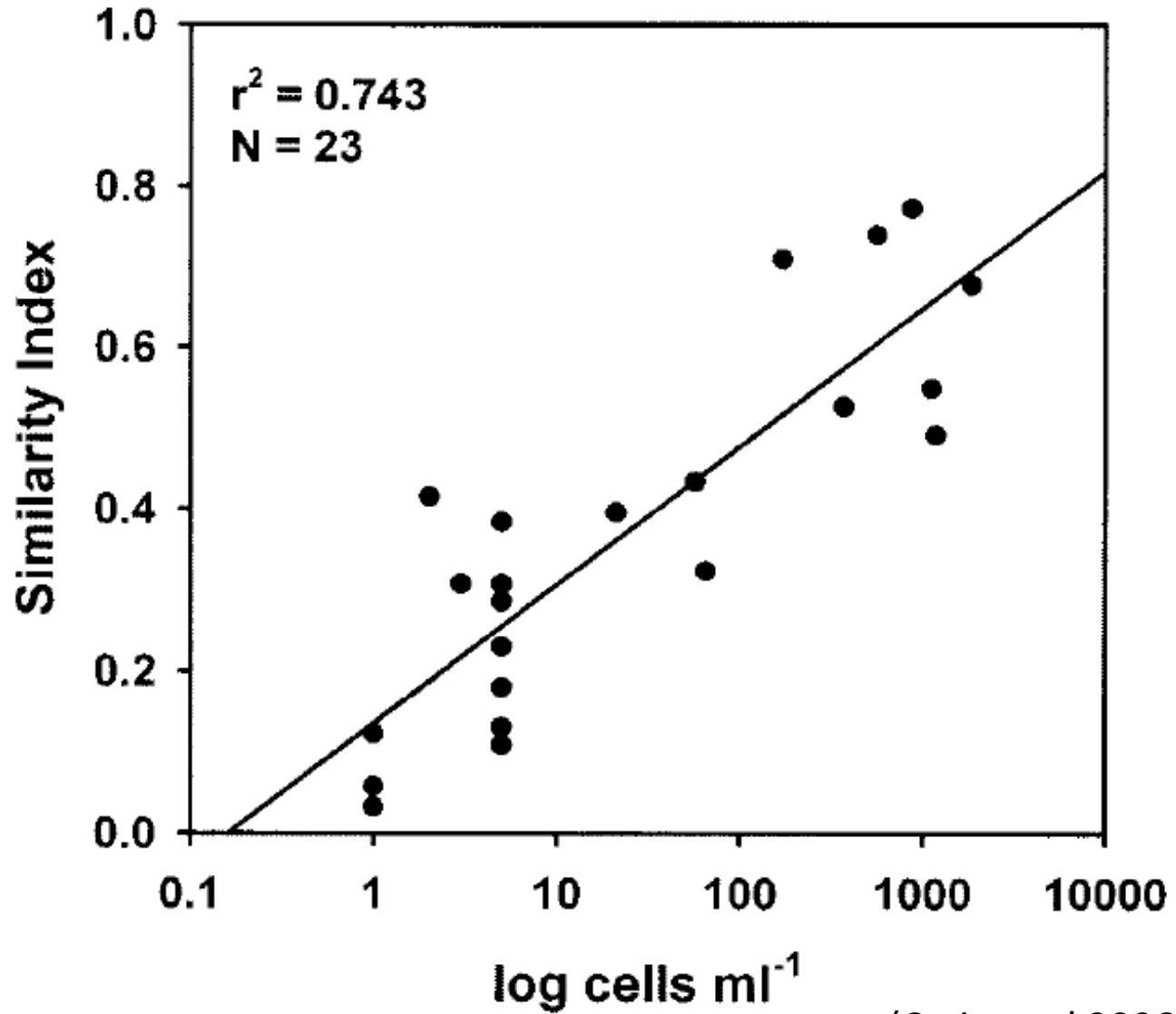
5c. HAB identification-2

$$R_{rs}(\lambda) \xrightarrow{\text{QAA}} a_{ph}(\lambda) = a(\lambda) - a_{dg}(\lambda) - a_w(\lambda)$$



(Lee and Carder 2004)

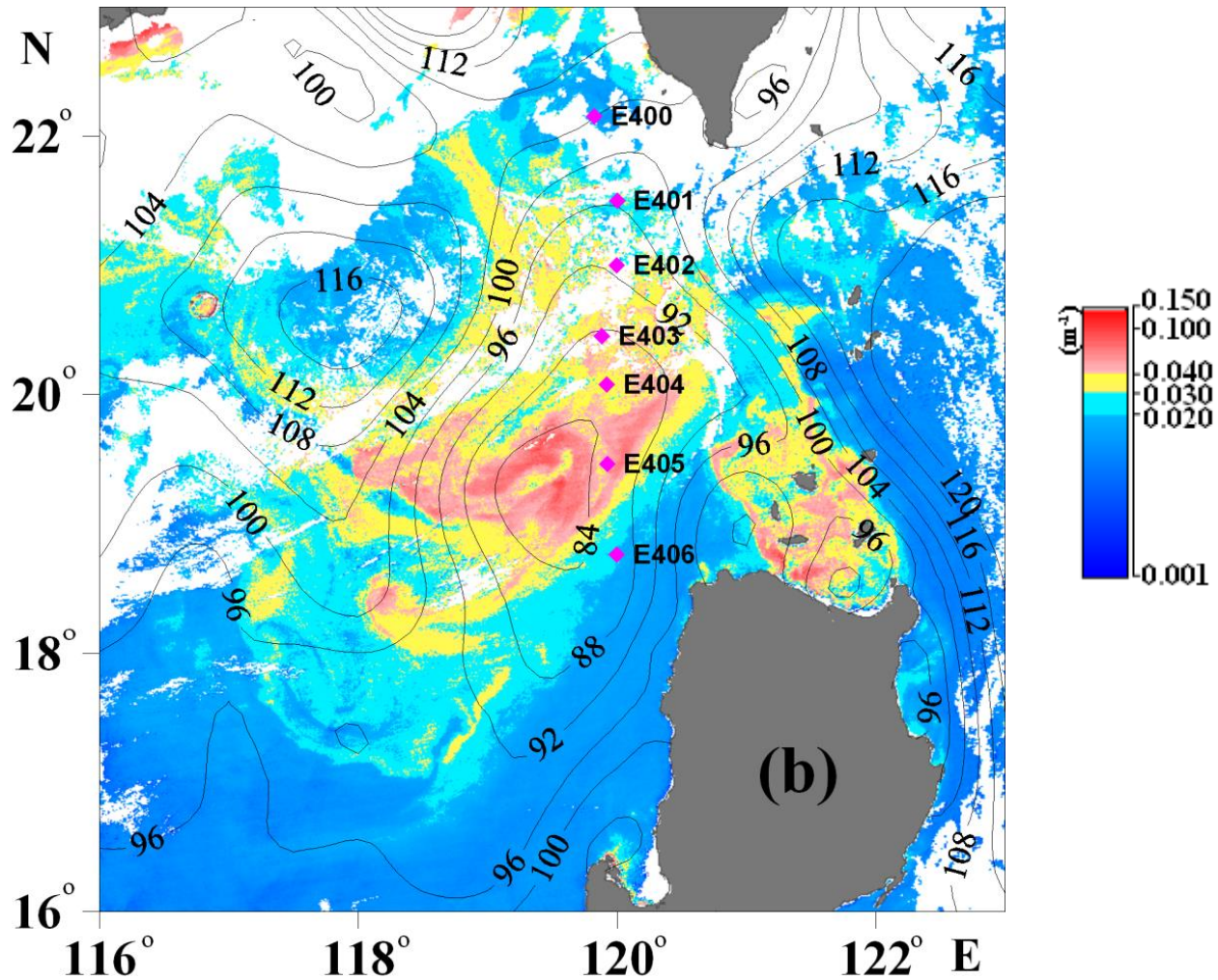
K. brevis



(Craig et al 2006)

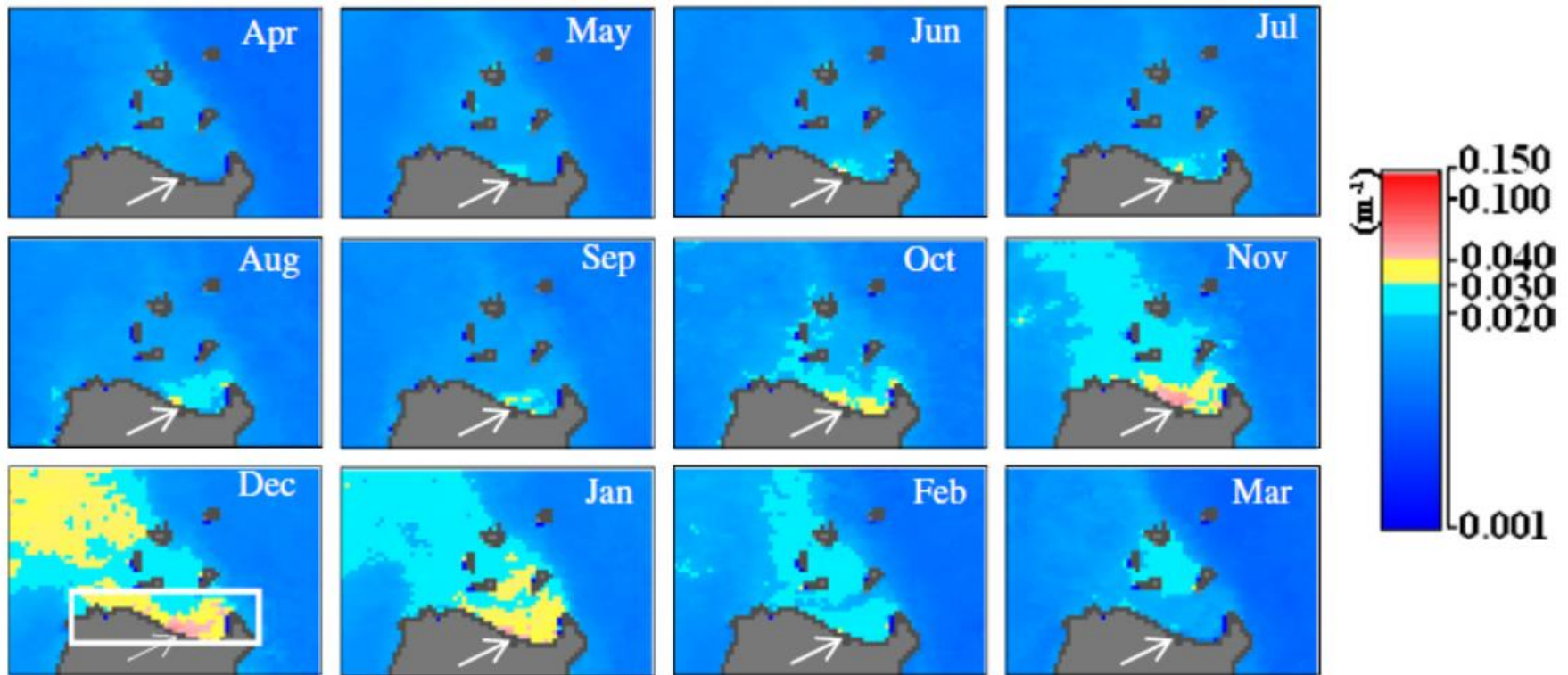
5d. Bloom dynamics

Distribution of $a_{ph}(440)$ at Luzon Street



(Shang et al, 2012)

Monthly distribution of $a_{ph}(440)$ at Luzon Street



(Shang et al, 2012)

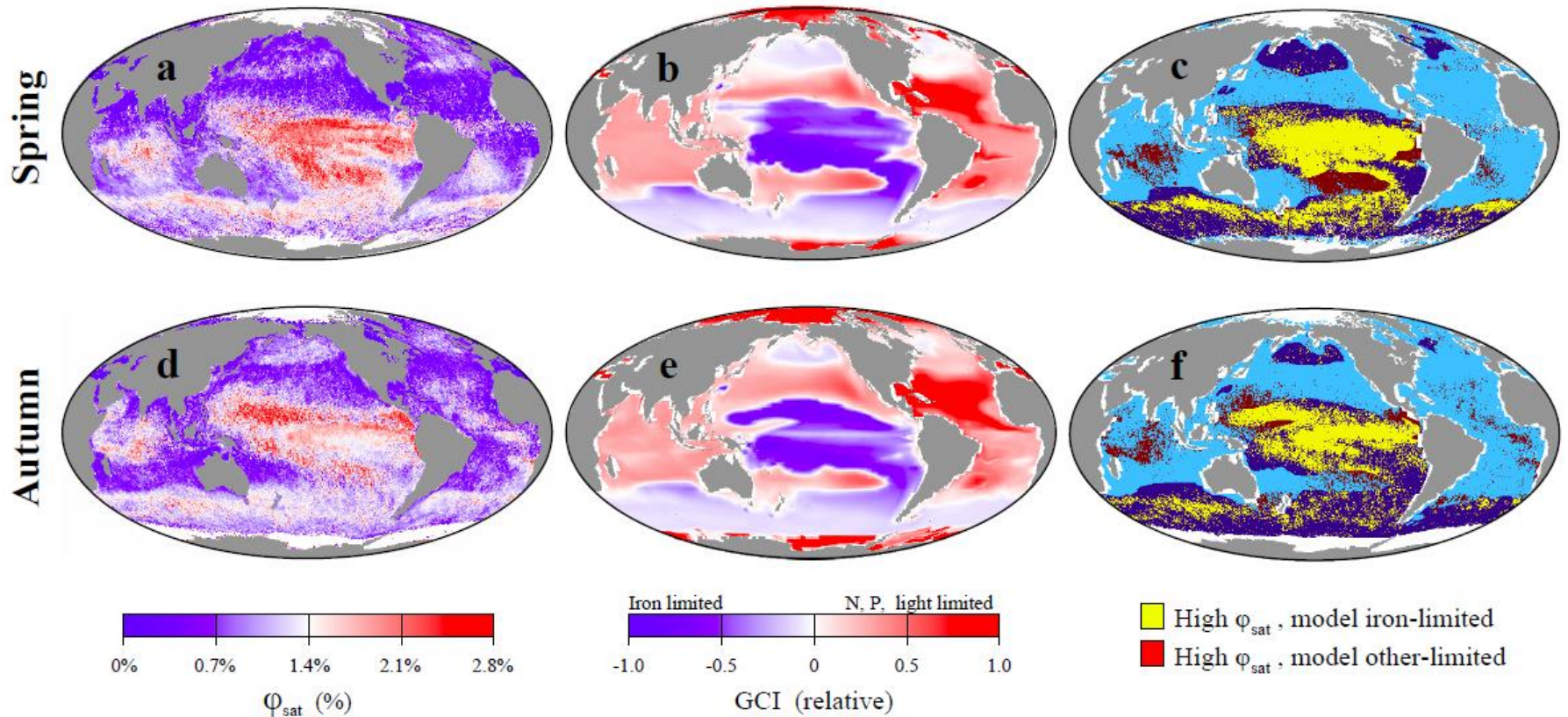
5e. Global physiology of ocean phytoplankton

IOP

$$F_{\text{sat}} = \text{Chl}_{\text{sat}} \times \langle a_{\text{ph}}^* \rangle \times \phi \times S, \quad (2)$$

ϕ : quantum yield of fluorescence

(Behrenfeld et al 2009)



(Behrenfeld et al 2009)

5f. Salinity estimation

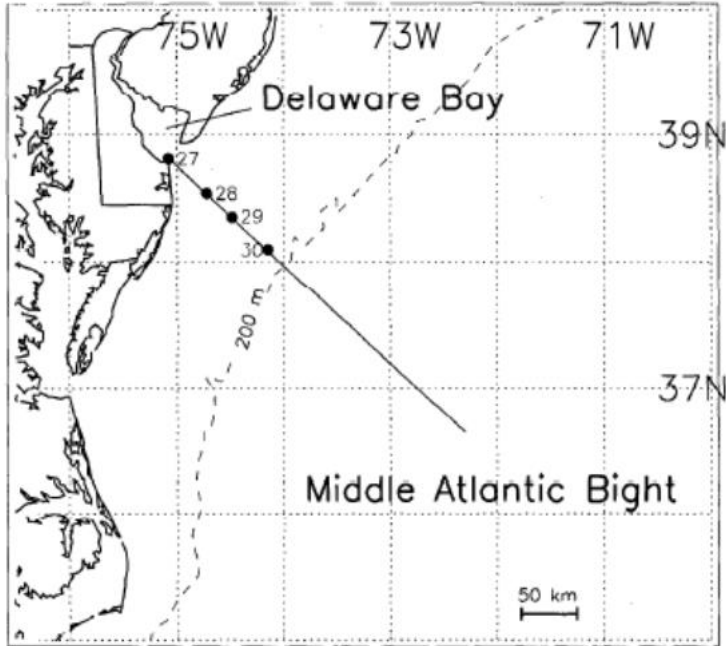
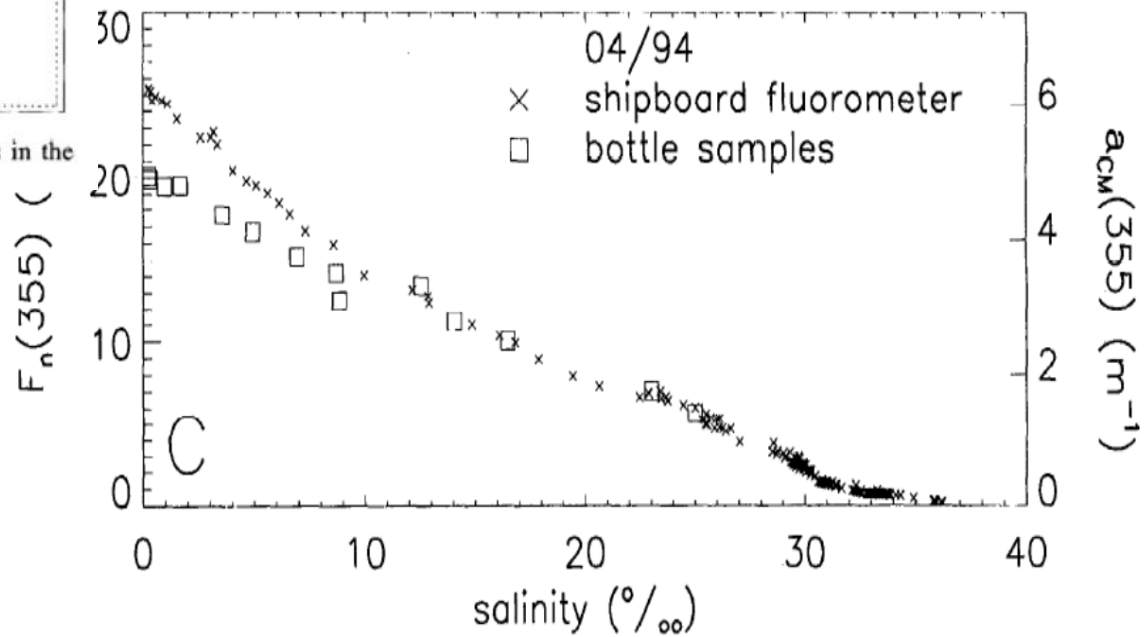
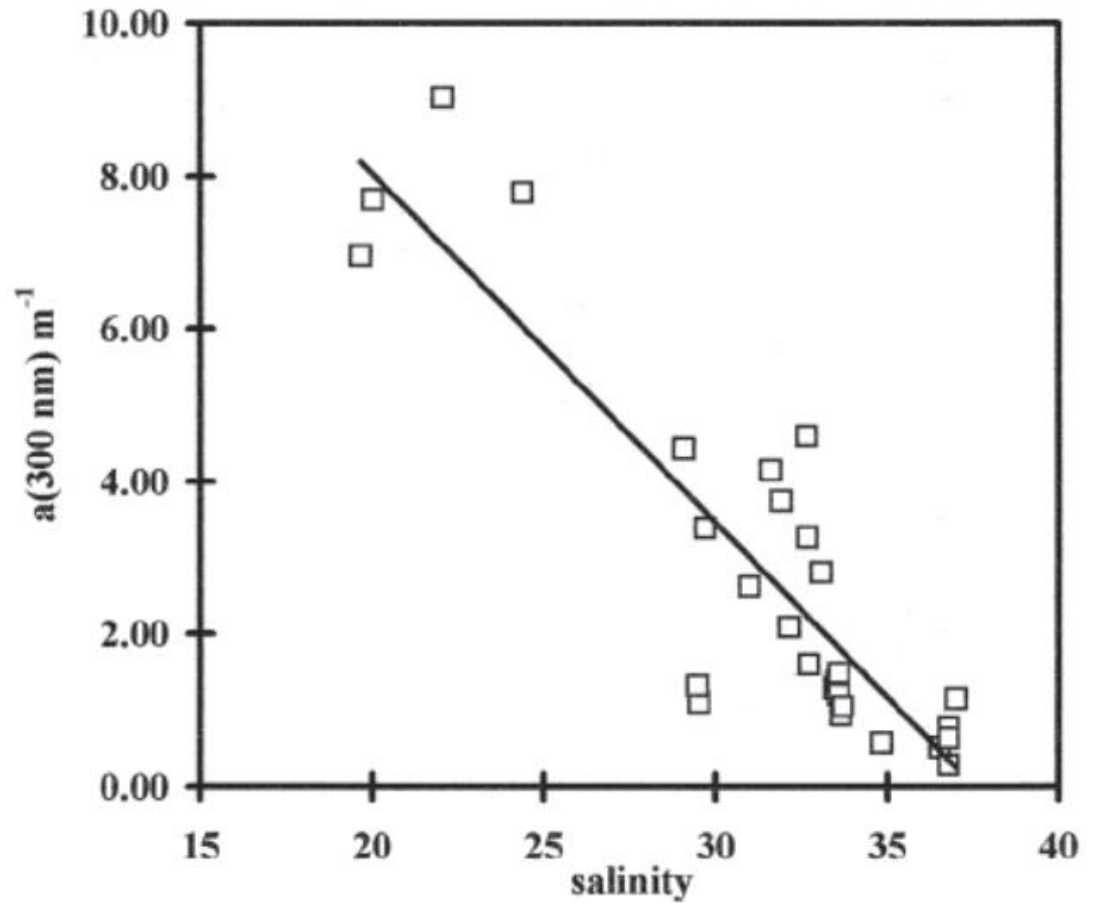
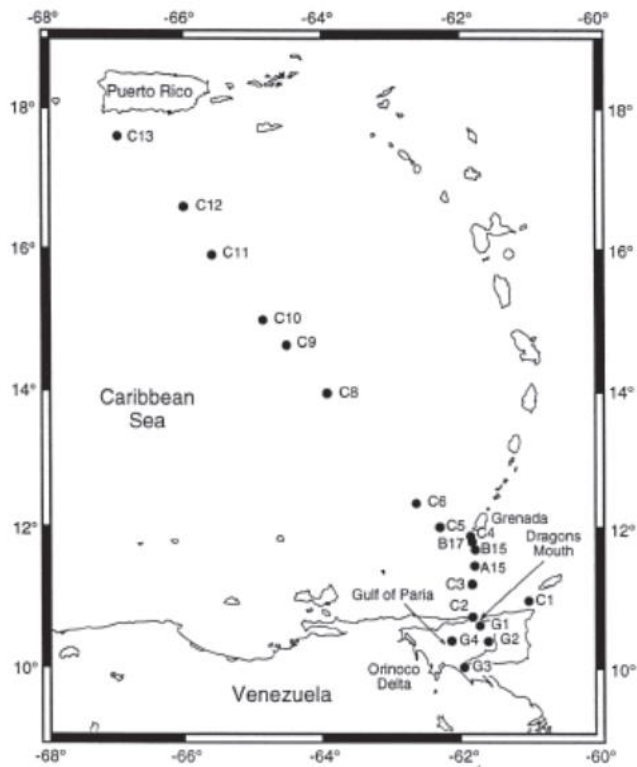


Fig. 1. Locations of the transect and hydrocast stations in the Middle Atlantic Bight.



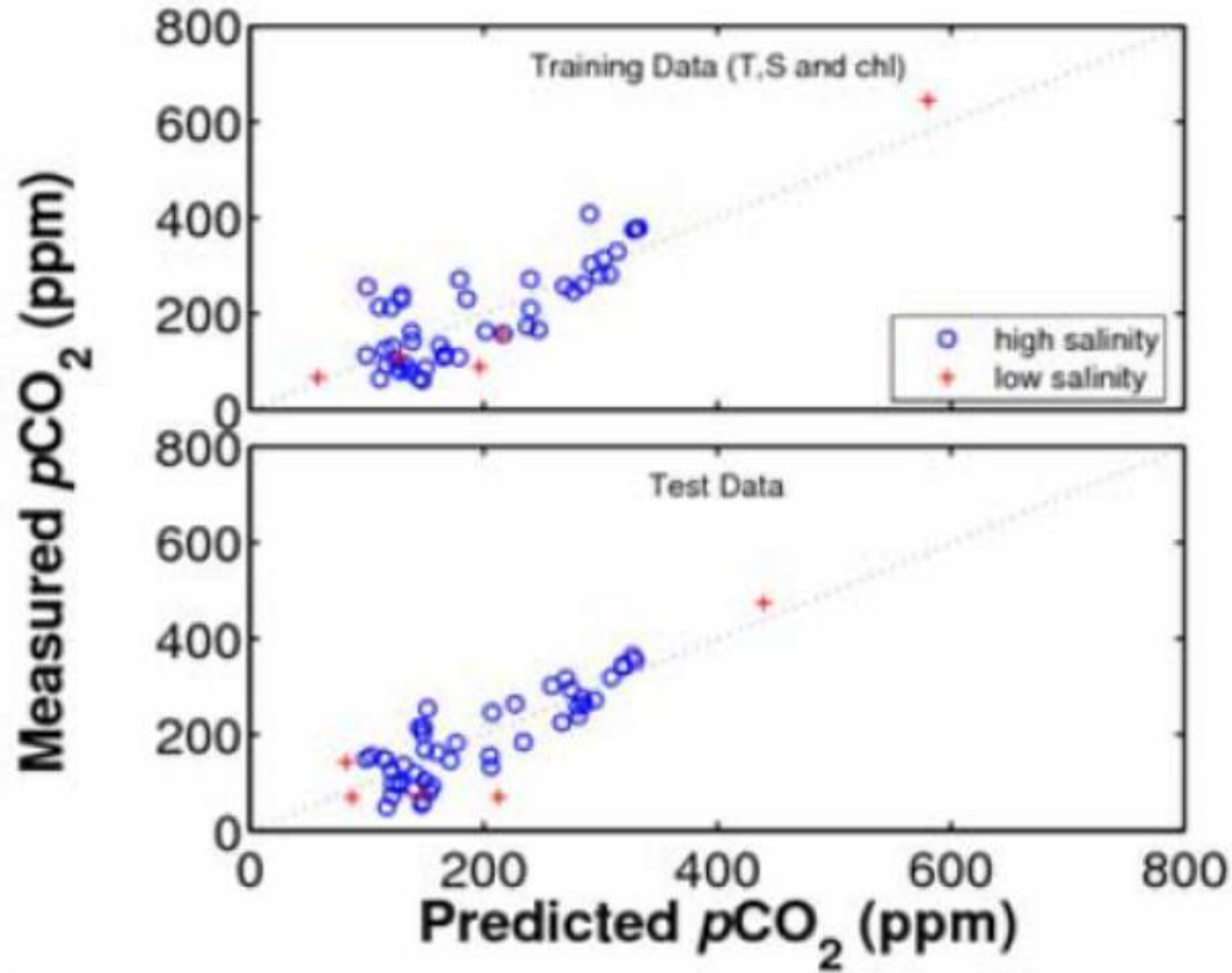
(Vodacek et al 1997)



$$SSS = X a_{\text{CDOM}} + Y$$

(Castellio et al 1999)

5g. pCO₂ estimation



Key Points:

1. Many applications traditionally built around remotely-sensed [Chl] can be built around remotely-sensed IOPs, and no need to limit to “Case-1” waters.
2. Remote sensing and applications centered around IOPs avoided, when necessary, concentration-normalized optical properties.
3. With IOPs as the inputs, many products, e.g. K_d , Z_{eu} , Z_{SD} , could be estimated semi-analytically and more accurately.
4. When IOPs are known, many other applications could be carried out. **Be creative.**

Thank you!

References:

THE DETERMINATION OF THE DIFFUSE ATTENUATION COEFFICIENT
OF SEA WATER USING THE COASTAL ZONE COLOR SCANNER

R.W. Austin and T.J. Petzold

J. F. R. Gower (ed.), *Oceanography from Space*
© Plenum Press, New York 1981

Bio-optical properties of oceanic waters: A reappraisal

André Morel

Laboratoire de Physique et Chimie Marines, Université Pierre et Marie Curie, CNRS-INSU
Villefranche-sur-mer, France

Stéphane Maritorena

JOURNAL OF GEOPHYSICAL RESEARCH, VOL. 106, NO. C4, PAGES 7163–7180, APRIL 15, 2001

An evaluation of MODIS and SeaWiFS bio-optical algorithms in the Baltic Sea

Mirosław Darecki^{a,*}, Dariusz Stramski^b

Remote Sensing of Environment 89 (2004) 326–350

Limnol. Oceanogr., 29(2), 1984, 350–356

© 1984, by the American Society of Limnology and Oceanography, Inc.

Dependence of relationship between inherent and apparent optical properties of water on solar altitude

J. T. O. Kirk

Limnol. Oceanogr., 34(8), 1989, 1389–1409

© 1989, by the American Society of Limnology and Oceanography, Inc.

Can the Lambert-Beer law be applied to the diffuse attenuation coefficient of ocean water?

Howard R. Gordon

Two-stream irradiance model for deep waters

Eyvind Aas

1 June 1987 / Vol. 26, No. 11 / APPLIED OPTICS

2095

A model for the diffuse attenuation coefficient of downwelling irradiance

Zhong-Ping Lee¹

Naval Research Laboratory, Stennis Space Center, Mississippi, USA

Ke-Ping Du

State Key Laboratory of Remote Sensing Science, Research Center for Remote Sensing and GIS, School of Geography, Beijing Normal University, Beijing, China

Robert Arnone

JOURNAL OF GEOPHYSICAL RESEARCH, VOL. 110, C02016, doi:10.1029/2004JC002275, 2005

Penetration of UV-visible solar radiation in the global oceans : Insights from ocean color remote sensing

Zhongping Lee,¹ Chuanmin Hu,² Shaoling Shang,³ Keping Du,⁴ Marlon Lewis,⁵ Robert Arnone,⁶ and Robert Brewin⁷

JOURNAL OF GEOPHYSICAL RESEARCH: OCEANS, VOL. 118, 4241–4255, doi:10.1002/jgrc.20308, 2013

Diffuse attenuation coefficient of downwelling irradiance: An evaluation of remote sensing methods

Zhong-Ping Lee,^{1,2} Mirosław Darecki,³ Kendall L. Carder,⁴ Curtiss O. Davis,⁵ Dariusz Stramski,⁶ and W. Joseph Rhea⁵

JOURNAL OF GEOPHYSICAL RESEARCH, VOL. 110, C02017, doi:10.1029/2004JC002573, 2005

Optical Modeling of the Upper Ocean in Relation to Its Biogenous Matter Content (Case I Waters)

ANDRÉ MOREL

JOURNAL OF GEOPHYSICAL RESEARCH, VOL. 93, NO. C9, PAGES 10,749–10,768, SEPTEMBER 15, 1988

Light and Photosynthesis in Aquatic Ecosystems ...

1994

Amazon.com: [Light and Photosynthesis in Aquatic Ecosystems](#): 9780521459662: Kirk, John

Penetration of solar radiation in the upper ocean: A numerical model for oceanic and coastal waters

ZhongPing Lee,^{1,2} KePing Du,³ Robert Arnone,¹ SooChin Liew,⁴ and Bradley Penta¹

JOURNAL OF GEOPHYSICAL RESEARCH, VOL. 110, C09019, doi:10.1029/2004JC002780, 2005

Reconciling Between Optical and Biological Determinants of the Euphotic Zone Depth

Jinghui Wu^{1,3} , Zhongping Lee² , Yuyuan Xie^{1,5} , Joaquim Goes³ , Shaoling Shang¹ ,
John F. Marra⁴ , Gong Lin¹, Lei Yang¹, and Bangqin Huang¹ 

RESEARCH ARTICLE


10.1029/2020JC016874

Light Penetration in the Coastal Waters Off Goa

SHUBHA SATHYENDRANATH & V V R VARADACHARI

Indian Journal of Marine Sciences
Vol. 11, June 1982, pp. 148-152

Resolving the long-standing puzzles about the observed Secchi depth relationships

Zhongping Lee ^{1*} Shaoling Shang ^{2*} Keping Du,³ Jianwei Wei ¹

Limnol. Oceanogr. 00, 2018, 00-00

Title:

The Visibility of Submerged Objects (Chapters 1 through 4)

Author:

[Duntley, Seibert Q](#)

Originally issued: August 1952

Reissued: October 1960

Secchi disk science: Visual optics of natural waters¹

Rudolph W. Preisendorfer

Limnol. Oceanogr., 31(5), 1986, 909–926

Robust underwater visibility parameter

J. Ronald V. Zaneveld

WET Labs, Inc., P.O. Box 518, Philomath, OR 97370

ron@wetlabs.com

W. Scott Pegau

17 November 2003 / Vol. 11, No. 23 / OPTICS EXPRESS 2997

Secchi depth in the Oslofjord–Skagerrak area: theory, experiments and relationships to other quantities

E. Aas¹, J. Høkedal², and K. Sørensen³

Ocean Sci., 10, 177–199, 2014

Ocean transparency from space: Validation of algorithms estimating Secchi depth using MERIS, MODIS and SeaWiFS data

Maéva Doron^{a,b,c,*}, Marcel Babin^{b,c}, Odile Hembise^a, Antoine Mangin^a, Philippe Garnesson^a

Remote Sensing of Environment 115 (2011) 2986–3001

Secchi disk depth: A new theory and mechanistic model for underwater visibility



ZhongPing Lee^{a,*}, Shaoling Shang^{b,*}, Chuanmin Hu^c, Keping Du^d, Alan Weidemann^e, Weilin Hou^e, Junfang Lin^a, Gong Lin^b

Remote Sensing of Environment 169 (2015) 139–149

A Decade of Satellite Ocean Color Observations*

Charles R. McClain

Annu. Rev. Mar. Sci. 2009. 1:19–42

IOCCG Report Number 2, 1999

**Status and plans for
Satellite Ocean-Colour
Missions: Considerations
for Complementary Missions.**

A consumer's guide to phytoplankton primary productivity models

Michael J. Behrenfeld and Paul G. Falkowski

Limnol. Oceanogr., 42(7), 1997, 1479–1491

Limnol. Oceanogr., 28(4), 1983, 770–776

© 1983, by the American Society of Limnology and Oceanography, Inc.

A simple, steady state description of phytoplankton growth based on absorption cross section and quantum efficiency¹

Estimating primary production at depth from remote sensing

Z. P. Lee, K. L. Carder, J. Marra, R. G. Steward, and M. J. Perry

20 January 1996 / Vol. 35, No. 3 / APPLIED OPTICS 463

An assessment of optical properties and primary production derived from remote sensing in the Southern Ocean (SO GasEx)

Zhongping Lee,¹ Veronica P. Lance,^{2,3} Shaoling Shang,⁴ Robert Vaillancourt,⁵

The Evolution of Optical

Water Mass Classification

BY ROBERT A. ARNONE, A. MICHELLE WOOD, AND RICHARD W. GOULD, JR.

Oceanography | June 2004

15

A novel technique for detection of the toxic dinoflagellate, *Karenia brevis*, in the Gulf of Mexico from remotely sensed ocean color data

Jennifer P. Cannizzaro^{a,*}, Kendall L. Carder^a, F. Robert Chen^a,
Cynthia A. Heil^b, Gabriel A. Vargo^a

Continental Shelf Research 28 (2008) 137–158

Absorption spectrum of phytoplankton pigments derived from hyperspectral remote-sensing reflectance

ZhongPing Lee^{a,*}, Kendall L. Carder^b

Remote Sensing of Environment 89 (2004) 361–368

Use of hyperspectral remote sensing reflectance for detection and assessment of the harmful alga, *Karenia brevis*

Susanne E. Craig, Steven E. Lohrenz, Zhongping Lee, Kevin L. Mahoney, Gary J. Kirkpatrick, Oscar M. Schofield, and Robert G. Steward

5414 APPLIED OPTICS / Vol. 45, No. 21 / 20 July 2006

Phytoplankton bloom during the northeast monsoon in the Luzon Strait bordering the Kuroshio

Shaoling Shang^{a,b,*}, Li Li^c, Jun Li^a, Yonghong Li^a, Gong Lin^a, Jun Sun^d

Remote Sensing of Environment 124 (2012) 38–48

Satellite-detected fluorescence reveals global physiology of ocean phytoplankton

M. J. Behrenfeld¹, T. K. Westberry¹, E. S. Boss², R. T. O'Malley¹, D. A. Siegel³, J. D. Wiggert⁴, B. A. Franz⁵, C. R. McClain⁵, G. C. Feldman⁵, S. C. Doney⁶, J. K. Moore⁷, G. Dall'Olmo¹, A. J. Milligan¹, I. Lima⁶, and N. Mahowald⁸

Biogeosciences, 6, 779–794, 2009

Seasonal variation of CDOM and DOC in the Middle Atlantic Bight:
Terrestrial inputs and photooxidation

Anthony Vodacek¹ and Neil V. Blough¹

Department of Chemistry and Biochemistry, University of Maryland, College Park, Maryland 20742

Michael D. DeGrandpre,² Edward T. Peltzer, and Robert K. Nelson

Limnol. Oceanogr., 42(4), 1997, 674–686

Analysis of the optical properties of the Orinoco River plume by
absorption and fluorescence spectroscopy

Carlos E. Del Castillo ^{a,*}, Paula G. Coble ^a, Julio M. Morell ^b, José M. López ^b,
Jorge E. Corredor ^b

Marine Chemistry 66 (1999) 35–51

**Satellite ocean color assessment of air-sea fluxes of CO₂ in a
river-dominated coastal margin**

Steven E. Lohrenz

Department of Marine Science, University of Southern Mississippi, Stennis Space Center, Mississippi, USA

Wei-Jun Cai

GEOFYSICAL RESEARCH LETTERS, VOL. 33, L01601, doi:10.1029/2005GL023942, 2006